DISSERTATIONES
TECHNOLOGIAE
CIRCUMIECTORUM
UNIVERSITATIS
TARTUENSIS
40

SHARVARI SUNIL GADEGAONKAR

Microbial and environmental factors affecting the nitrate removal efficiency from water in bioelectrochemical systems

DISSERTATIONES TECHNOLOGIAE CIRCUMIECTORUM
UNIVERSITATIS TARTUENSIS
40

DISSERTATIONES TECHNOLOGIAE CIRCUMIECTORUM
UNIVERSITATIS TARTUENSIS
40

SHARVARI SUNIL GADEGAONKAR

Microbial and environmental factors affecting the nitrate removal efficiency from water in bioelectrochemical systems

UNIVERSITY OF TARTU
Press
1632

Department of Geography, Institute of Ecology and Earth Sciences, Faculty of Science and Technology, University of Tartu, Estonia

This dissertation has been accepted for the commencement of the degree of Doctor of Philosophy in Environmental Technology at the University of Tartu on June 5th, 2023, by the Scientific Council on Environmental Technology, Faculty of Science and Technology, University of Tartu.

Supervisors: Prof. Ülo Mander
Institute of Ecology and Earth Sciences, Department of Geography
University of Tartu
Estonia

Associate Prof. Mikk Espenberg
Institute of Ecology and Earth Sciences, Department of Geography
University of Tartu
Estonia

Opponent: Dr. Jamie Nivala
Senior Scientist and Director of research
INRAE
France

Commencement: Senate Hall, University Main Building, Ülikooli 18, Tartu, on August 23rd, 2023, at 10.15.

Publication of this dissertation is granted by the Institute of Ecology and Earth Sciences, University of Tartu.

ISSN 1736-3349 (print)
ISBN 978-9916-27-286-2 (print)
ISSN 2806-2612 (pdf)
ISBN 978-9916-27-287-9 (pdf)

University of Tartu Press
www.tyk.ee

TABLE OF CONTENTS

ORIGINAL PUBLICATIONS

This thesis is based on the following publications which are referred to in the text by Roman numerals. Published papers are reproduced in print with the permission of the publisher.

I. **Gadegaonkar, S.S**., Philippon, T., Rogińska, J., Mander, Ü., Maddison, M., Etienne, M., Barrière, F., Kasak, K., Lust, R., Espenberg, M. 2020. Effect of cathode material and its size on the abundance of nitrogen removal functional genes in microcosms of integrated bioelectrochemical-wetland systems. Soil Systems 4(3), 47. https://doi.org/10.3390/soilsystems4030047

II. Lust, R., Nerut, J., **Gadegaonkar, S.S.,** Kasak, K., Espenberg, M., Visnapuu, T., Mander, Ü. 2022. Single-chamber microbial electrosynthesis reactor for nitrate reduction from waters with a low electron donors' concentration: from design and set-up to the optimal operating potential. Frontiers in Environmental Sciences 10, 938631. https://doi.org/10.3389/fenvs.2022.938631

III. **Gadegaonkar, S.S.,** Mander, Ü., Espenberg, M. 2023. A state-of-the-art review and guidelines for enhancing nitrate removal in bio-electrochemical systems (BES). Journal of Water Process Engineering. https://doi.org/10.1016/j.jwpe.2023.103788

Author's contribution to the articles denotes: '*' a moderate contribution, '**' a major contribution.

Categories	Articles		
	I	II	III
Original idea	**	*	**
Study design	*	*	**
Data processing and analysis	**	**	**
Interpretation of the results	**	**	**
Writing the manuscript	**	*	**

Department of Geography, Institute of Ecology and Earth Sciences, Faculty of Science and Technology, University of Tartu, Estonia.

ABBREVIATIONS AND ACRONYMES

BES	Bio-electrochemical system
MES	Microbial electrochemical snorkel
MESR	Microbial electrosynthesis reactor (1 chambered; low carbon)
MFC	Microbial fuel cell
CW-BES	Constructed wetland conjugated bio-electrochemical system
CFU	Colony forming units
TC	Total carbon
TOC	Total organic carbon
DOC	Dissolved organic carbon
DC	Dissolved carbon
DN	Dissolved nitrogen
TN	Total nitrogen
DNA	Deoxyribonucleic acid
RNA	Ribonucleic acid
amoA	Ammonia monooxygenase
nirS	Nitrite reductase cytochrome cd_1-Nir
nirK	Nitrite reductase Cu-Nir
nosZI	Nitrous oxide reductase clade I
nosZII	Nitrous oxide reductase clade II
narG	Nitrate reductase subunit alpha
ANAMMOX	Anaerobic ammonium oxidation
DNRA	Dissimilatory nitrate reduction to ammonium
COMAMMOX	Complete ammonia oxidation
nrfA	Nitrite reductase representing DNRA
qPCR	Quantitative Polymerase Chain Reaction
N_2	Dinitrogen
N	Nitrogen
NH_4^+	Ammonium
NH_4OH	Ammonium hydroxide
NO_3^-	Nitrate
NO_2^-	Nitrite
N_2O	Nitrous oxide
N_2	Dinitrogen
GHG	Greenhouse Gas
SO_4^{2-}	Sulfate
WE	Working electrode
CE	Counter electrode
SHE	Standard hydrogen electrode
CV	Cyclic Voltammetry

ABSTRACT

Bioelectrochemical systems (BES) have been recognized as an attractive technology for treating nitrate (NO_3^-) contaminated water. BES heavily rely on microbial processes to carry out the reduction of NO_3^- in conjugation with the electrochemical reduction. We investigated the gene abundances of N transforming processes to determine the prevalent processes responsible for NO_3^- removal in BES. Microbial electrochemical snorkel systems (MES) were studied to determine the influence of cathode material and its' size on NO_3^- removal rates, the sustainability of MES was investigated by N_2O flux measurements, the N transforming gene abundances, cyclic voltammetry to determine the reduction potential and physiochemical parameters were tested for thorough observation of the MES. MES removal efficiencies were 40% to 70% and ~98% for NO_3^- and nitrite (NO_2^-) removal, respectively. The short circuit significantly reduced the gene abundances, therefore, altering the microbial activity. The graphite felt treatments supported nitrifiers but curbed *nirK*-possessing denitrifiers. The anaerobic ammonium oxidation (ANAMMOX) activity showed a decline compared to the controls. Higher N_2O fluxes were displayed with 1:1 cathode:anode and treatments using graphite felt, copper, plastic and stainless steel. *nirS* and *nosZI* genes have displayed a significant rise in numbers and are mainly responsible for the production and consumption of N_2O fluxes, respectively. *nrfA* gene representing the dissimilatory NO_3^- reduction to ammonium (NH_4^+) (DNRA) process was widely enhanced with electrochemical manipulation and may be responsible for N_2O fluxes. The single-chambered microbial electrosynthesis reactor (MESR) displayed stable NO_3^- removal rates. A larger CE (counter electrode) compared to WE (working electrode) aided in maintaining the pH (~7.3) and a lower oxygen (O_2) concentration in the system. The higher NO_3^- concentration and a potential of −756 mV initiated NO_3^- reduction in MESR. The maximum NO_3^- removal rate of 3.8±1.2 mg N-NO_3^- L^{-1} day^{-1} was achieved at −656 mV at a faradic efficiency of 71%. The abundances of *nir* and *nosZ* genes were higher on WE compared to the CE, indicating the presence of denitrifiers in the system and, therefore, denitrification being responsible of NO_3^- removal. The share of heterotrophic microbes was ~5%, which is indicative for the autotrophic denitrification driving the process, as this was a carbon-deficient MESR. DNRA process was observed in MESR, likely causing ~45% of NO_3^- conversion to NH_3 at certain potential; indicated by the detection of *nrfA* gene abundances on WE. We investigated the BES components and operational parameters on their importance on the NO_3^- removal efficiency. The removal efficiencies of NO_3^- were assessed by considering various factors, including electrode materials, working mode, number of chambers, inoculum type, capacity, and microbial community structure. In particular, electrode materials had a significant impact on the rate of NO_3^- removal. When employing the random forest classifier algorithm, operational parameters such as working mode, number of chambers, inoculum type, and BES capacity were found to be important factors that significantly influenced NO_3^- removal

efficiencies. The dominant phyla observed in BES treating NO_3^- contaminated water was *Proteobacteria* and *Firmicute*. In addition to the denitrification process, characterized by the abundance of *narG, nirS, nirK, nosZI*, and *nosZII* genes, there was evidence of electrochemical support for ANAMMOX (represented by the abundance of *hzsB* or ANAMMOX-specific 16S rRNA genes) and DNRA (indicated by the abundance of *nrfA* gene) processes in BES. Based on our analysis, a continuous two-chamber BES system with granular carbon and carbon paper as cathode and anode materials, respectively, and denitrifying microbes as the inoculum type, would contribute to optimal NO_3^- removal efficiencies.

Thus, BES have greater potential in reducing NO_3^- and carrying out complete denitrification as denitrifiers are resilient to electrochemical manipulation. BES can also be exploited for enhanced DNRA processes for the recovery of nitrogen (N) or can be utilized for successful NO_3^- removal at carbon-deficient waters such as groundwater and have larger application in mitigation of NO_3^- removal.

1. INTRODUCTION

1.1 Nitrate as an evolving minacious pollutant

Nitrogen (N) is the most abundantly found element in the atmosphere (78%). It can be naturally fixed by certain microbial communities on the planet for utilization of different living beings. Atmospheric N_2 can be converted to various reactive forms such as ammonium (NH_4^+), nitrite (NO_2^-), nitrate (NO_3^-), and nitrous oxide (N_2O). N is an essential element and an integral part of the building blocks of different biomolecules. Though, through the advent of the Haber-Bosch process it has been artificially fixed in huge volumes on the planet. N has been rapidly used for the production of fertilizers in large quantities. The imbalance in the N cycle i.e. large volumes fixed and not completely removed from the environment has caused a threat to the terrestrial, coastal, and marine life forms (Galloway et al., 2008). Excessive NO_3^- is a stable form of N and is recognized as a major pollutant. Unmanaged NO_3^- has contaminated various water bodies leading to eutrophication and consumption of NO_3^- contaminated water causes methemoglobinemia (the blue baby syndrome). N cycle imbalances have surpassed the defined threshold determined for the scope of humanity on this planet (Rockström et al., 2009).

The limit for drinking water concentration of NO_3^- is 50 mg-NO_3^-/L according to the EU and WHO, and 44.3 mg NO_3^-/L set by the United States Environmental Protection Agency. The groundwater is majorly contaminated due to the diffused agricultural run-off, rich in NO_3^-. Around 60% of rural areas in Asia and Africa rely on groundwater for their major water requirements (Margat and van der Gun et al., 2013). The global nitrogen fixed is around 413 Tg of reactive nitrogen (Nr) in terrestrial and marine ecosystems, on which anthropogenic activities are 210 Tg (Fowler et al., 2013). The chemically fixed N is mostly utilized for the production of N fertilizers, to meet the exponential demand of food production.

1.2 Nitrogen cycle and nitrogen transforming communities

N is the limiting element on the planet and all living organisms rely on nitrogen as an essential macronutrient, though nitrogen is present in abundance as dinitrogen (N_2), majority of the organisms can assimilate it in the form of NH_4^+ or NO_3^-. The N cycle consists of primarily assimilation, ammonification, nitrification, denitrification, anaerobic ammonium oxidation (ANAMMOX), and nitrogen fixation. The N-transforming microorganisms carry enzymes that perform 14 redox reactions involving 8 key inorganic nitrogen species of different oxidation states (Kuypers et al., 2018) ($NH_4^+ \rightarrow NH_2OH \rightarrow NO_2^- \rightarrow NO_3^- \rightarrow NO_2^- \rightarrow N_2O \rightarrow N_2$) (Fig. 1).

N is fixed from the atmosphere on the planet by bacteria and archaea which possess an enzyme nitrogenase metalloenzyme and can fix N_2 to NH_3. These

enzymes are dependent on a metal cofactor for their functioning and consist of three types i.e. iron-iron (FeFe), vanadium-iron (VFe), and molybdenum-iron (MoFe). *nifH* is used as a genetic marker for the detection of N-fixing microbes. Ammonia oxidation to hydroxylamine is carried out by aerobic ammonia-oxidizing bacteria and archaea using ammonia monooxygenase (AMO) (Arp et al., 2003). Hydroxylamine oxidation to nitric oxide and eventually to nitrite is carried out aerobically by octahaem hydroxylamine oxidoreductase (HAO) (Schalk et al., 2009). Nitrite oxidation to nitrate is catalyzed by nitrite oxidoreductase (NXR) harbored by aerobic nitrite-oxidizing bacteria and anaerobic ammonium-oxidizing bacteria (Daims et al., 2011). Nitrate reduction to nitrite is called dissimilatory nitrate reduction which is carried out by organisms from all domains of life and catalyzed by membrane-bound or periplasmic nitrate reductase (NAP) (Sparacino-Watkins et al., 2013). Nitrite reduction to ammonium is used for both assimilatory and dissimilatory purposes, performed by octahaem tetrathionate reductase (ONR) or the octahaem nitrite reductase (ONR) and plasmic cytochrome c nitrite reductase encoded by *nrfAH* (Sparacino-Watkins et al., 2013; Campeciño et al., 2020). Nitrite reduction to nitric oxide is carried out by anaerobic ammonium-oxidizing bacteria, the reaction is catalyzed by haem-containing cd_1 nitrite reductase (*nirS*) or a Cu-containing nitrite reductase (*nirK*) (Li et al., 2013). The primary process that reduces the amount of the potent greenhouse gas N_2O through microorganisms involves converting it into N_2 gas. This transformation is facilitated by the nitrous oxide reductase (NOS) enzyme, which is the only known catalyst for this reaction. Anaerobic ammonium oxidation (ANAMMOX) refers to the process of converting ammonium to dinitrogen gas, which occurs without oxygen and uses NO_2^- as the final electron acceptor (Bernhard et al., 2010).

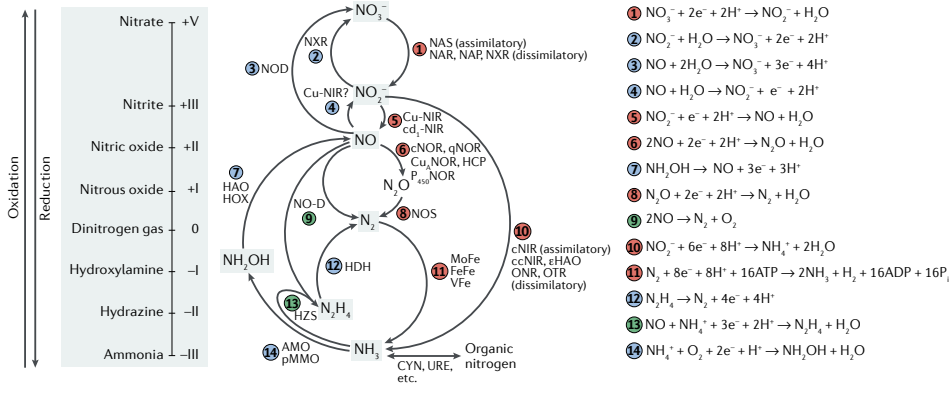

Fig. 1. The above figure displays the nitrogen transforming processes, physiochemical conditions, genes responsible and the balanced chemical reactions involved (Kuypers et al., 2018).

1.3 Bioelectrochemical systems (BES)

Microorganisms transfer electrons from a lower potential to a higher potential. BES is applied for electricity generation or utilized for their reduction reaction with a certain potential poised by electron transfer. BES can be classified as: Microbial fuel cell (MFC), consists of micro-organisms acting as biocatalysts for electricity generation in which the electrons generated due to internal metabolism i.e. substrate oxidation is transferred from the anode and finally captured by the cathode electrode via an external circuit. The biofilm formed on the surface of the electrodes promotes electron transfer (Conners et al., 2022). Microbial electrolytic cells (MEC), consists of micro-organisms inoculated in a cathode chamber which transfer the electrons to the cathode thus, accelerating the intracellular reduction metabolism (Rousseau et al., 2020). MECs act reverse of the MFCs as in the process of transfer of electrons from anode to cathode in an MFC the substrate is reduced while in MECs the potential poised on the cathode is determined by the electron shuttles and bacteria as they possess different potential differences. Microbial electrochemical snorkel (MES) is a short-circuited MFC, it doesn't produce any power but works at maximum potential as there is no voltage between the electrodes (Hoareau et al., 2019). The utilization of BES for nitrogen removal is recently explored, due to its enhancing reductive abilities they can be more suitable for complete nitrogen removal in comparison to the conventional biological methods (Su et al., 2022). Application of BES in the combination of physiochemical and biological treatment can augment the process of NO_3^- removal. To aid complete denitrification constructed wetlands conjugated with BES (CW-BES) are extensively studied, because due to the dynamic anoxic conditions, diffused agricultural pollution and low carbon concentration observed in constructed wetland denitrification is incomplete or inhibited. Whereas, BES provided contained conditions for optimum NO_3^- removal (Lu et al., 2008).

AIMS AND OBJECTIVES

The effectiveness of bioelectrochemical systems (BES) in removing NO_3^- primarily relies on the microbial community structure, which is influenced by the BES environment. However, there is still much to learn about the prevalent processes causing N-transformation in BES and their relationship to the environment of the BES, as it remains an understudied area.

The main aim of this study was to analyze microbial and environmental factors affecting the NO_3^- removal efficiency in bioelectrochemical systems. Figure 2 and 3 represent the main conceptual aspects of this study.

Following specific objectives support to achieve the main aim:

- ✓ Executing a thorough study on BES specifically treating NO_3^- in order to observe the nitrogen transforming community.
- ✓ Determining the NO_3^- removal efficiency of the systems.
- ✓ Studying two different kinds of BES: Microbial snorkel systems (MES) and single-chambered microbial electrosynthesis reactor (MESR) treating carbon-deficient NO_3^--contaminated water.
- ✓ Examining the NO_3^- removal efficiencies of the systems by electrochemical and microbial studies.
- ✓ Determining the prevalent processes responsible for NO_3^- removal.
- ✓ Generating a thorough dataset of BES treating NO_3^- contaminated water and examining the influence of varying parameters on the NO_3^- removal rates.
- ✓ Determining the most crucial parameters for NO_3^- removal in BES using feature selection.
- ✓ Determining the influences of the physiochemical parameters on the NO_3^- removal.
- ✓ Examining the sustainability of the systems.

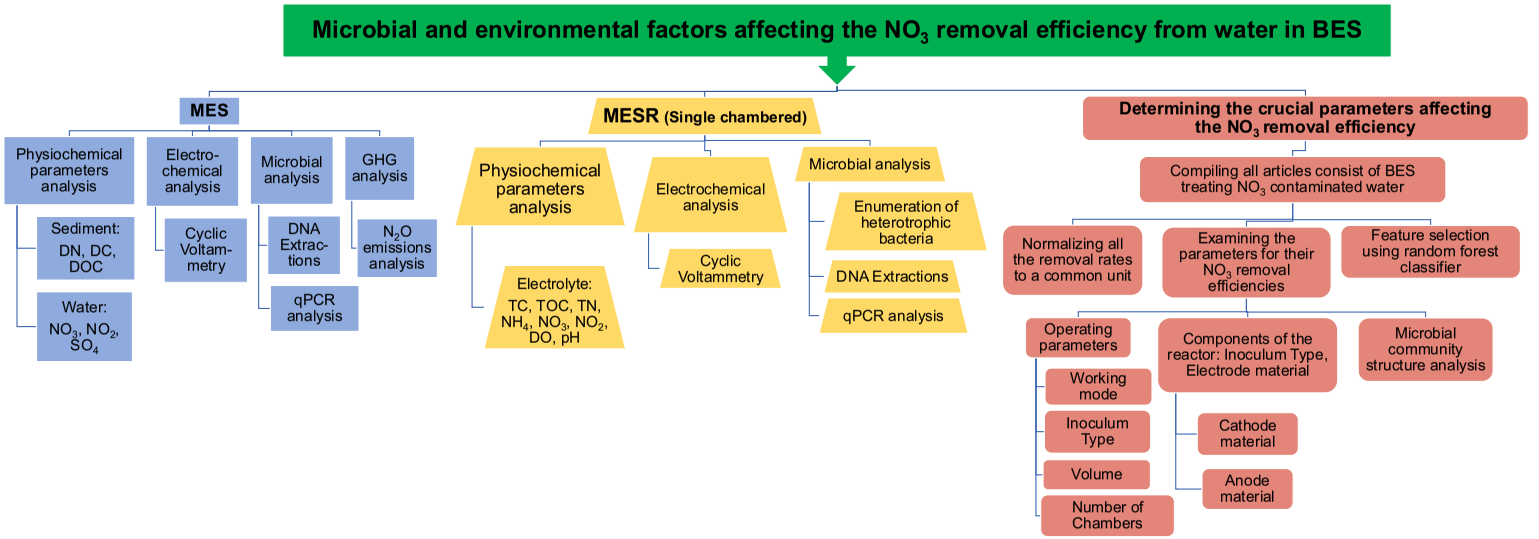

Fig. 2. Conceptual view of microbial and environmental factors affecting the NO_3^- removal efficiency in bio-electrochemical systems (BES).

2. MATERIAL AND METHODS (Publications I–III)

2.1 Data Collection and classification (Article III)

To examine articles investigating the use of BES for NO_3^- removal, data was collected from the Google Scholar search engine and the NCBI database, between March 2022 and March 2023. Various search terms, such as 'bio-electrochemical system', 'biocathode', 'denitrification', 'DNRA' and 'ANAMMOX' 'microbial community', and 'nitrate removal', were used either alone or in combinations, in singular or plural forms. To ensure a comprehensive search, all references cited in the collected papers were also examined. The analysis included papers published up until March 2023, and a total of 75 individual observations were included. The papers were chosen based on specific criteria, such as the use of BES for NO_3^- removal, inclusion of different types of BES (MFCs, MESs, and CW-BES), availability of NO_3^- removal rates and percentages, and relevance of information for calculating these rates and percentages (Appendix Tables A and B) (Fig. 3).

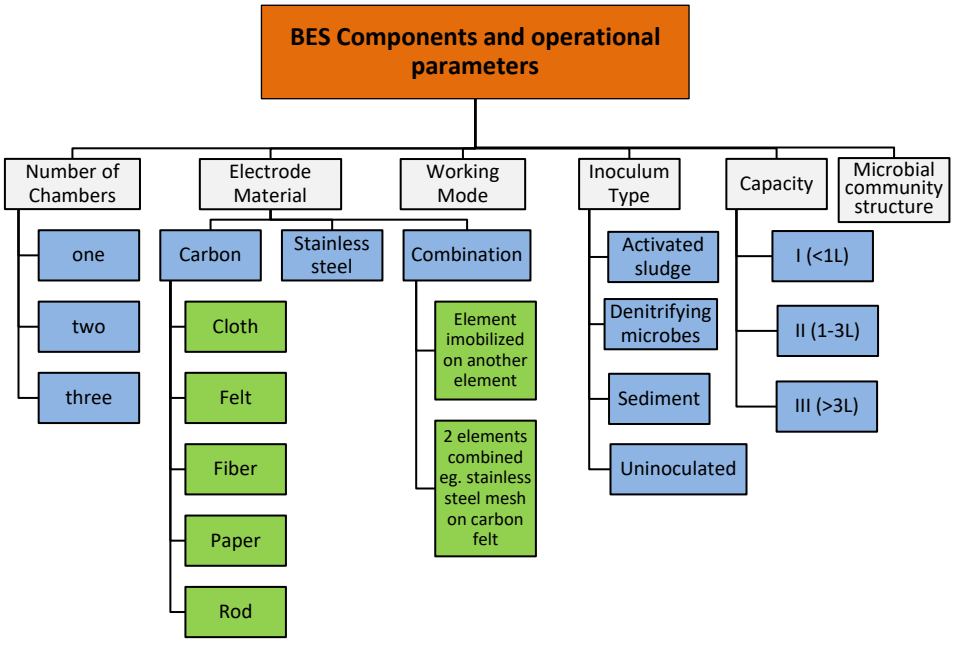

Fig. 3. Components and operational parameters of bio-electrochemical systems (BES).

2.2 Design of reactors

The two reactors studied were a microbial electrochemical snorkel (MES) and a single chambered microbial electrosynthesis reactor (MESR) utilized for treating carbon rich and carbon-deficient NO_3^- contaminated water respectively.

As, there are several acronyms defining the reactors, for the thesis purposes they will be denoted as MES for reactor 1 (Article I) and MESR for reactor 2 (Article II).

2.2.1 Reactor 1- Microbial Electrochemical Snorkel (MES) (Article I)

MES was build using plastic buckets with a volume of 2L and the height of 13 cm, diameter of 10.5 cm. The sediment from the Vantaa constructed wetland was filled up to 7 cm of the bucket. The anodes were embedded at bottom of the reactor, while the cathode rested on the sediment (Fig. 4). The anode and the cathode are connected by stainless steel wires using copper tape. The electrodes were connected in shortcut. Every treatment was carried out in triplicates and total 27 MES were constructed (Table. 1).

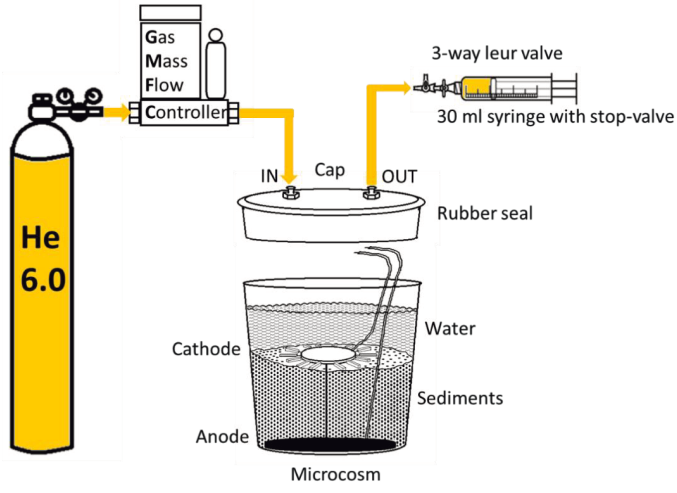

Fig. 4. The assembly of MES (Article I).

Table. 1. The treatments of MES.

Cathode: Anode	1:1	1:2	1:4	
Cathode material	Graphite felt	Copper	Plastic	Stainless Steel
Controls	No cathode	No electrodes		

2.2.2 Reactor 2- Microbial Electrosynthesis Reactor (MESR) (Article II)

Single chambered 5.86L plexiglass single chambered microbial electrosynthesis reactor (MESR) were constructed, to decrease the oxygen production on the counter electrode (CE) was 3.6 times larger surface area compared to the working electrode (WE). The graphite felt was used for both CE and WE. There were two inlet and outlets connected via pump for circulation of the electrolyte (Fig. 5). Titanium wire and graphite-based powder mixed with epoxy in a ratio of 1:1 connected cathode and anode electrodes. The reactors were operated as 3-electrode systems with reference electrodes (REs). *T. denitrificans* was inoculated in the reactor to aid in denitrification. Total of 3 reactors with varying treatments were run. Reactor 1-Working MESR inoculated with *T. denitrificans,* Reactor 2-Control MESR with NO_3^- water and Reactor 3- Abiotic MESR, sterilized electrolyte and surface sterilized reactor.

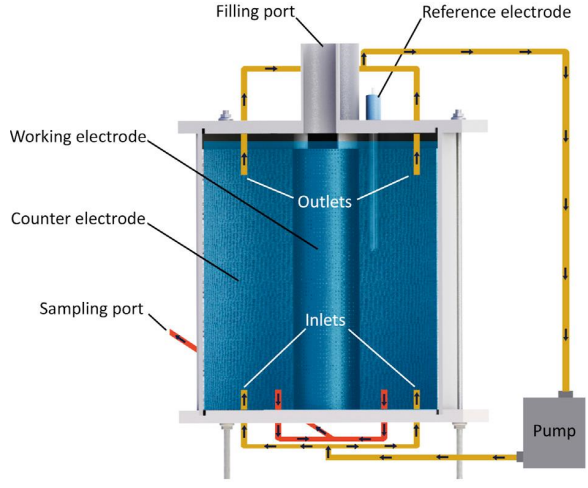

Fig. 5. The single chambered MESR assembly (Article II).

2.3 Operating parameters for the reactors

2.3.1 MES (Article I)

In order to simulate NO_3^--rich waters, 50 mg N-NO_3^-/L was added to the reactors on days 9, 13, and 24. The electrodes were not subjected to any external polarization and were instead left in short circuit. The systems were run in a dark room at room temperature for 45 days.

Small fragments of cathodes from each pilot were collected and examined through cyclic voltammetry using a potentiostat (910 PSTAT mini Metrohm) in a three-electrode configuration cell, with a stainless-steel rod used as the counter electrode. The reference electrode utilized was Ag/AgCl (+0.197 V vs. SHE) and the scan rate was 1 mV s^{-1}. Only the second cycle was recorded, with the samples studied in a 0.1 M sodium chloride electrolyte prepared in pure water that was degassed with helium bubbling before the experiment to eliminate dissolved oxygen. The cyclic voltammograms were recorded prior to and after the addition of 10 mM sodium nitrate ($NaNO_3^-$) to assess the potential for NO_3^- bioelectrochemical reduction by microbes on the cathode surface. The cathode and anode electrode polarizations were measured every other day in each pilot by submerging a reference electrode into the sediment and measuring the potential between the reference electrode and the cathode or anode electrode with a multimeter. Two different reference electrodes were employed during the experiment: Ag/AgCl (+0.197 V vs. SHE) and saturated calomel electrode (SCE +0.244 V vs. SHE). To simplify data comparison, the polarizations were converted against SHE.

2.3.2 MESR (Article II)

When the reactor was constructed and loaded with synthetic wastewater, N_2 was used to purge the reactor until the dissolved oxygen (DO) concentration decreased below 0.2 mgO_2/L, the concentration that aids microbial NO_3^- reduction. Before each cycle began, the electrolyte level was adjusted to the 5.5 L mark, and the NO_3^- concentration was raised to 100 mgN-NO_3^-/L by adding KNO_3^-, unless otherwise specified. The cycles were referred to as "cycle (1:2, 3:1)" throughout the study, with the first digit representing the reactor, and the second digit indicating the number of cycles performed in that reactor. Each cycle concluded when the NO_3^- was depleted or no changes in concentration were observed.

2.4 Chemical analysis (Articles I and II)

EVS-EN 1484 standard was used for determining the total carbon (TC), total inorganic carbon (TIC) and total organic carbon (TOC). Total nitrogen (TN) was determined utilizing the EVS-EN 12260 standard using the Vario TOC cube (Elementar Analysensysteme GmbG, Langenselbold, Germany).

Water samples were measured for NO_3^-, NO_2^- and SO_4^{2-}, using Ion chromatograph Metrohm 930 compact IC Flex, column used was Metrosep A Supp5 1004.0 with the effluent consisting of 1.0 Mm $NaHCO_3$ and 3.2 Mm Na_2CO_3.

The WTW Multi 3420 equipment from Xylem Analytics in Singapore was used to determine DO, pH, and temperature levels. The WTW FDO 925 tool was utilized for DO measurements, the WTW pH-Electrode SenTix 940-3 for pH measurements, and the WTW FDO 925 for temperature measurements.

Water were sampled every three days for carrying out chemical analysis.

2.5 N_2O sampling and analysis (Article I)

The gas from the MES was collected using displacement technique using helium 6.0 which displaced the air in the reactor which was collected via syringe in an evaluated 30ml glass vial every 40 mins for 2 hours. The gas samples were analyzed using gas chromatography using electron capture detector (ECD) with Shimadzu GC-2014 and Loftfield's autosampler.

2.6 Calculation of the NO_3^- removal rate and the Faradaic efficiency (Article II)

The cycle consisted of three phases: the lag phase, stable phase, and end phase, each with different characteristics. Since the cycles were longer than 20 days, it was difficult to determine when NO_3^- was entirely depleted. Therefore, NO_3^- removal rates and Faradaic efficiency were calculated based on the stable phase data. The rate of NO_3^- reduction was determined by evaluating the amount of reduced NO_3^- per day.

$$Faradaic\ efficiency\ = (amount\ of\ NO3\ reduced\ in\ moles \times 5 *\div moles\ of\ electrons) \times 100$$

*5: The number of electrons required to reduce one NO_3^- according to half-reaction (Di Capua et al., 2019).

2.7 Microbial analysis

The sediment samples from MES were collected at the day 1 (start), day 18 (middle) and the day 45 (end) of the experiment for microbial analysis. Three sets of electrodes were collected from MESR for microbial analysis (Table. 2).

Table. 2. The table displays the cycles the electrode sets participated and the day they were collected for microbial analysis during the course of the MESR run.

Name	Electrodes	Day	Cycles
Reactor 1	Set 1	612	1:1–1:8
Reactor 2	Set 2	169	2:2–2:5
Reactor 3	Set 3	30	3:1

2.7.1 DNA extraction (Articles I and II)

0.25g of the samples were homogenized and utilized for DNA extraction using the PowerSoil DNA Isolation kit ((MO BIO Laboratories Inc, Carlsbad, CA, USA), the homogenization was carried out at 5000rpm for 20s. The DNA concentration measured was carried out using Infinite M200 spectrophotometer and the samples were stored at −20 °C.

2.7.2 Quantitative Polymerase Chain Reaction (qPCR) (Articles I and II)

qPCR analysis assays were carried using the RotorGene Q machine and the quantification of the genes was carried out using the RotorGene Series Software v.202 and LinRegPCR program v.2020. The abundances of the gene copies per gram dry weight (copies/g dw). The sum of the bacterial and archaeal 16S rRNA represent the proportion of the prokaryotic community. The primers and the program utilized for gene amplification are displayed (Table. 3).

Table. 3. Primer sets utilized for gene amplification and the qPCR program.

	Primers	Primer concentration (M)	Amplicon size (bp)	qPCR program	Reference
Bacterial 16S rRNA	Bact517F / Bact1028R	0,6	530	95 °C 10 min; 35 cycles: 95 °C 30 s; 60 °C 45 s; 72 °C 45 s	Liu et al., 2007 / Dethlefsen et al., 2008
Archaeal16S rRNA	Arc519F / Arc910R	0,6	393	95 °C 10 min; 45 cycles: 95 °C 15 s; 56 °C 30 s; 72 °C 30 s	Espenberg et al., 2016
nirS	nirSCd3af / nirSC3cd	0,8	431	95 °C 10 min; 45 cycles: 95 °C 15 s; 55 °C 30 s; 72 °C 30 s; 80 °C 30	Kandeler et al., 2006
nirK	nirK876 / nirK1040	0,8	165	95 °C 10 min; 45 cycles: 95 °C 15 s; 58 °C 30 s; 72 °C 30 s; 80 °C 30	Hallin & Lindgren, 1999
nosZI	nosZ2F / nosZ2R	0,8	267	95 °C 10 min; 45 cycles: 95 °C 15 s; 60 °C 30 s; 72 °C 30 s; 80 °C 30	Henry et al., 2006
nosZII	nosZIIF / nosZIIR	1,2	~700	95 °C 10 min; 45 cycles: 95 °C 30 s; 54 °C 45 s; 72 °C 45 s; 80 °C 45	Jones et al., 2013
Bacterial *amoA*	amoA-1F / amoA-2R	0,8	491	95 °C 10 min; 45 cycles: 95 °C 30 s; 57 °C 45 s; 72 °C 45 s	Rotthauwe et al., 1997
Archaeal *amoA*	CrenamoA 23F / CrenamoA 616R	0,8	~600	95 °C 10 min; 45 cycles: 95 °C 30 s; 54 °C 45 s; 72 °C 45 s	Touma et al., 2008
COMAMMOX *amoA*	comamoA AF / comamoA SR	0,8	436	95 °C 10 min; 40 cycles: 95 °C 15 s; 55 °C 30 s; 72 °C 30 s	Wang et al., 2018
ANAMMOX 16S rRNA	A438F / A684R	0,6	248	95 °C 10 min; 45 cycles: 95 °C 15 s; 52 °C 30 s; 72 °C 30 s	Humbert et al., 2012
nrfA	6F / 6R	0,8	222	95 °C 10 min; 45 cycles: 95 °C 15 s; 55 °C 30 s; 72 °C 30 s	Takuchi, 2006
nifH	Ueda19F / Ueda407R	0,8	390	95 °C 10 min; 45 cycles: 95 °C 30 s; 53 °C 45 s; 72 °C 45 s	Ueda et al., 1995

2.7.3 *Thiobacillus denitrificans* culture preparation (Article II)

Thiobacillus denitrificans possesses all the necessary genes for the denitrification process. Accordingly, a thriving culture of *Thiobacillus denitrificans* was obtained from DSMZ (German Collection of Microorganisms and Cell Cultures GmbH, Leibniz Institute, Brunswick, Germany) and utilized as an inoculum during the second experiment (Article III). The culture was propagated in accordance with the instructions provided by the supplier using medium 113 (German Collection of Microorganisms and Cell Cultures GmbH, Leibniz Institute, Brunswick, Germany) in three phases. Initially, 5 mL of culture was cultivated in a 25 mL medium. After three days, the inoculum was diluted by adding 270 mL of fresh medium. Thirty days later, the inoculum was further diluted by adding 200 mL of medium. Ten days following this, the inoculum was agitated, and 200 mL of the inoculum was employed for each reactor.

2.7.4 Determination of heterotrophic microbes for MESR (Article II)

To count the number of microorganisms in the electrolyte during the 1:3 cycle, samples were taken from the reactor and stored in sterile containers at 4 °C. Viable cell count was performed within 4 hours using decimal dilution series with dilution factors ranging from 101 to 106. The ISO 6222:1999 standard method was used for culturable microorganism enumeration in water samples. Colony counts were recorded after 3–4 days at 22 °C and 2–3 days at 37 °C, and the results from longer time points were used in calculations due to slow colony growth. The number of colony-forming units (CFU) per 1 mL of the initial water sample was calculated from 4 to 6 parallel plates at each time point of the reactor process. The number of denitrifying bacteria was determined using the most probable number (MPN) method. Decimal dilutions with dilution factors from 101 to 104 were inoculated into Hiltay medium, and inoculum sizes of 1 mL were applied to 10 mL Hiltay test tubes. The number of positive test tubes showing pH shift and nitrogen gas formation was recorded, and MPN indexes were used to calculate the MPN per 1 mL of the initial water sample using the MPN calculator (MPN calc v1.2.0). All inoculations were performed in two technical parallels for colony counts and three replicates for MPN indexes.

2.8 Statistical analysis

2.8.1 Article I and II

R version 3.6.3 (R Core Team, 2020) was utilized to explore, standardize, scrutinize, and display the data. Multivariate linear models were built to examine the significance of differences among the investigated treatments regarding physicochemical variables, gene parameters, and emission values. The ANOVA function in R package mvabund v. 4.1.3 was used to test the constructed models. The correlation between target gene parameters and environmental factors was evaluated using Spearman's rank correlation coefficients. The p-values were adjusted for the false discovery rate using the Benjamini-Hochberg method with significance levels of $p<0.05$ and $p<0.01$. The correlation networks were visualized using Cytoscape v. 3.7.2.

2.8.2 Article III

The data was analyzed and visualized using the software R version 4.2.1. Feature selection was performed using the Boruta package version 8.0 (Kursa and Rudnicki et al., 2010), which uses the random forest classification algorithm to identify important parameters for model building. Boruta determines the statistical significance and importance of the parameters used in building and running the BES. ANOVA was conducted to determine the statistical significance of the varying groups of parameters, and pairwise comparisons between groups were performed using the post hoc Tukey's HSD (honestly significant difference) test.

3. RESULTS

3.1 NO_3^- removal efficiencies in BES

3.1.1 Electrode material for optimum NO_3^- removal efficiencies

Our study focused on exploring which electrode materials display high NO_3^- removal efficiencies. The cathode materials included in our dataset were stainless steel, combination electrodes, and carbon in different forms such as cloth, felt, fiber, granules, paper, and rod. Carbon, especially graphite felt, was the most commonly used cathode material in our dataset (as shown in Table A and B). Our findings showed that the NO_3^- removal efficiency differed significantly among the various cathode electrode materials ($p<0.01$). The highest NO_3^- removal rates were observed with carbon granules followed by carbon paper. However, there was a greater variation in the removal rates with carbon granules and carbon paper compared to the other cathode materials, which showed less variability in their removal efficiencies (Fig. 6a).

The materials tested for the anode in our study included stainless steel, combination electrodes, and carbon in various forms such as cloth, felt, mesh, fiber, granules, paper, and rod. Among the anode materials tested, carbon paper had the highest removal efficiency and showed less variation in removal rates compared to other anode materials (Fig.6b). Our analysis revealed significant differences in removal rates among the various anode types ($p<0.05$).

The highest removal rates were displayed with materials imparting higher surface areas for NO_3^- removal i.e. carbon granules as cathode material and paper as anode material. The higher surface area aids in harboring the microbial community structure and could be attributed to the higher NO_3^- removal efficiencies.

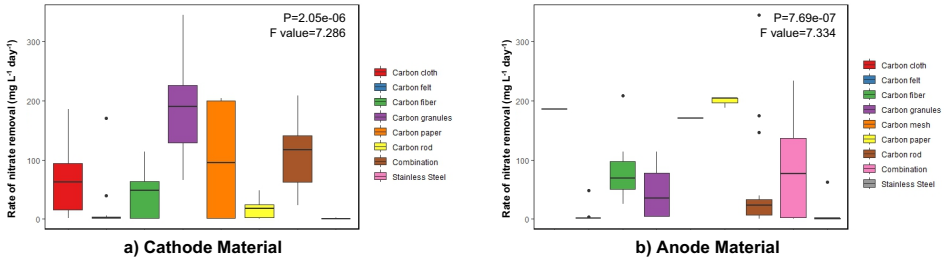

Fig. 6. Box plots representing different cathode (a) and anode (b) materials compared to the NO_3^- removal rate (Article III).

3.1.2 Effect of cathode material and size on NO_3^- removal efficiencies in MES

High degree of variability in NO_3^- removal efficiency was observed across different treatments. Plastic cathodes exhibited the highest NO_3^- removal efficiency, followed by control and no cathode systems. In contrast, all other systems demonstrated slightly lower NO_3^- removal efficiency, which was slightly <50%. However, NO_2^- removal efficiency was found to be very high (>98%) across all the studied systems (Fig. 7; Table. 4).

Electrochemical manipulation has displayed influence on the NO_3^- removal rates compared to control systems, plastic electrodes just aid surface area for the microbial community as it's a non-conductive material but has displayed higher removal rates compared to other treatments. There is significant difference between water NO_3^- concentrations among varying treatments, the temporal dynamics of the NO_3^- and NO_2^- display similar patterns in all treatments.

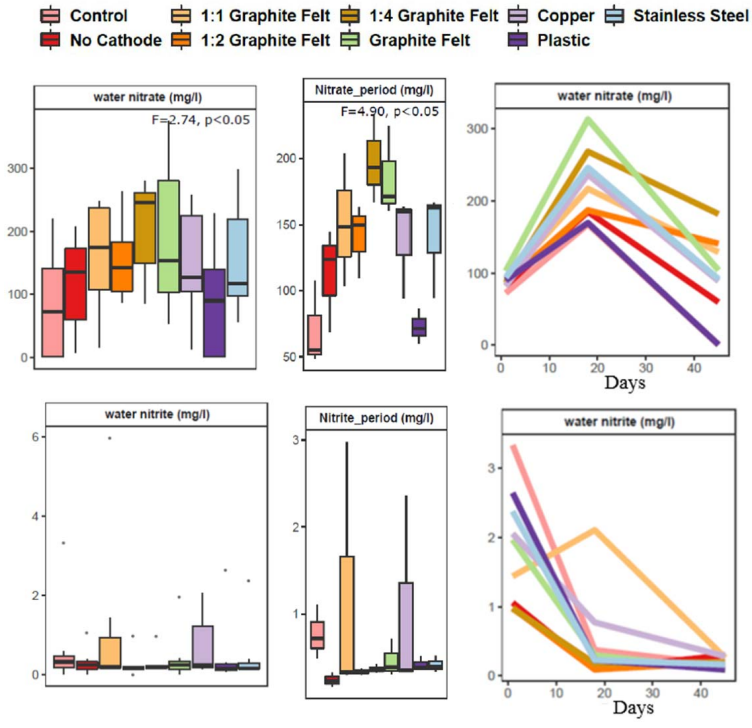

Fig. 7. The box plots display the water concentrations for NO_3^- and NO_2^-, concentrations over the period of experiment and temporal dynamics respectively.

Table. 4. Average ± standard deviation (n = 3) of NO_3^- and NO_2^- removal efficiency (%) (Article I).

Treatment	Nitrate Removal	Nitrite Removal
Control	66.51 ± 1.54	98.66 ± 0.42
No Cathode	53.88 ± 23.52	99.37 ±0.08
1:1 Graphite Felt	48.39 ± 29.05	98.07 ± 2.31
1:2 Graphite Felt	41.35 ± 15.27	99.40 ± 0.06
1:4 Graphite Felt	41.52 ± 6.99	99.33 ± 0.11
Graphite Felt	41.18 ± 13.67	99.00 ± 0.20
Copper	40.55 ± 26.70	99.39 ± 0.27
Plastic	74.61 ± 7.22	99.39 ± 0.27
Stainless steel	40.34 ± 9.88	99.25 ± 0.22

3.1.3 The optimum potential for NO_3^- removal in MESR

In MESR, the WE potential was set to −320 mV with an initial NO_3^- concentration of 14.6 mg N-NO_3^-/L. NO_3^- concentrations remained unchanged until day 36 when NO_3^- concentrations were increased to 82.4 and 70.8 mg N-NO_3^-/L for reactors 1 and 2, respectively. The WE potential was then lowered after every 3–7 days by 50 mV, and then increased to +43 mV, which was the anodic potential, but no NO_3^- reduction occurred. The WE potential was lowered to −756 mV, and on day 186, the NO_3^- concentration drop was registered from 82.4 mgN-NO_3^-/L to 50 mgN-NO_3^-/L (Fig. 8). The NO_3^- reduction in Reactor 1 was driven by the applied current, and NO_3^- was completely reduced in 43 days in cycle (1:2) with KNO_3^- added. The study revealed the competition between autotrophic denitrification and DNRA and 49% of NO_3^- was reduced to NH_4^+.

Overall, the NO_2^- concentration remained negligible throughout the experiment, whereas there was generation of NH_4^+ which can be visualized in Fig. 9.

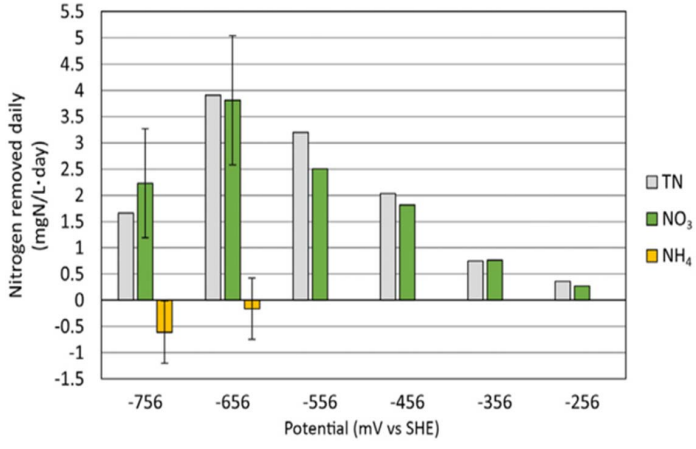

Fig. 8. Relationship between the electrode potential (mV vs. standard hydrogen electrode), nitrogen removal rate. Daily removal rate for total nitrogen (TN), NO_3^-, NH_4^+ on different WE potentials (Article II).

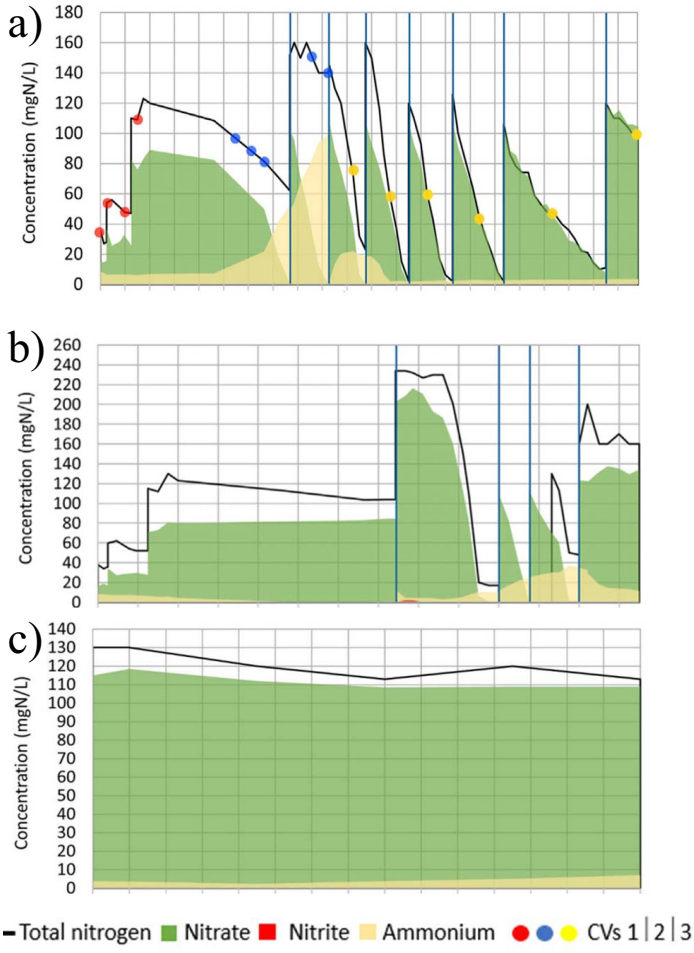

Fig. 9. The electrolyte's TN, NO_3^-, NO_2^-, and NH_4^+ concentrations are shown in an area graph, with red, blue, and yellow dots indicating when the CV measurements were conducted. a, b, c – represent measurements of Reactor 1,2 and 3 respectively.

3.2 Physiochemical parameters in the MES and MESR

MES treatments showed significant differences in sediment DC and DOC values ($p<0.05$ and $p<0.01$, respectively). Controls had different temporal trends compared to other treatments for DC, DOC values (Fig. 10). High carbon concentrations were observed mid experiment, the carbon concentrations declined as the experiment progressed. The rise in the DOC denotes the growth of microbes in the MES and indicative of the NO_3^- utilized as a substrate. The eventual decline in the carbon concentration would be attributed to the presence of heterotrophic microbes or the effect of electrochemical manipulation on the microbial load.

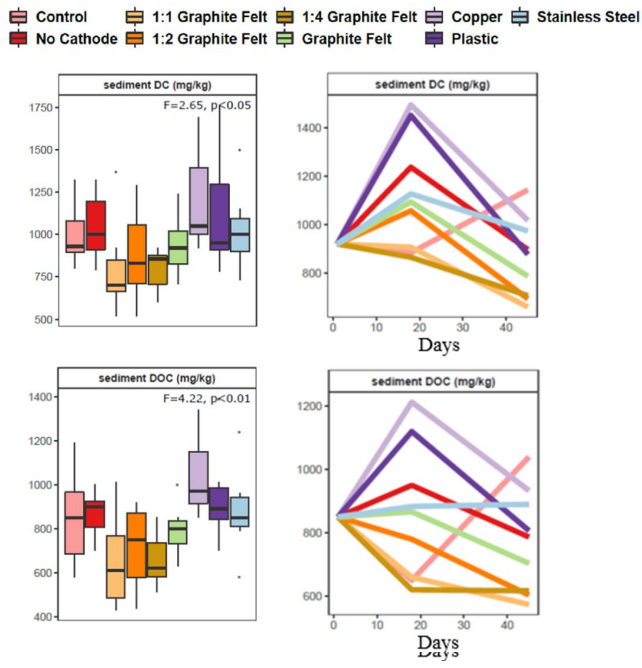

Fig. 10. The box plots display the sediment concentrations for DC and DOC, and temporal dynamics respectively.

Sulfate concentrations in water were significantly different between MES treatments ($p<0.01$, respectively), sulfate concentrations have significant difference between treatments over the course of the experiment ($p<0.05$) (Fig. 11). There is a consistent accumulation of sulfate observed over the period in MES, which can be attributed to the utilization of inorganic sulfur compounds such as thiosulfate ($S_2O_2^{-3}$), hydrogen sulfide (H_2S) etc. by autotrophic denitrifiers.

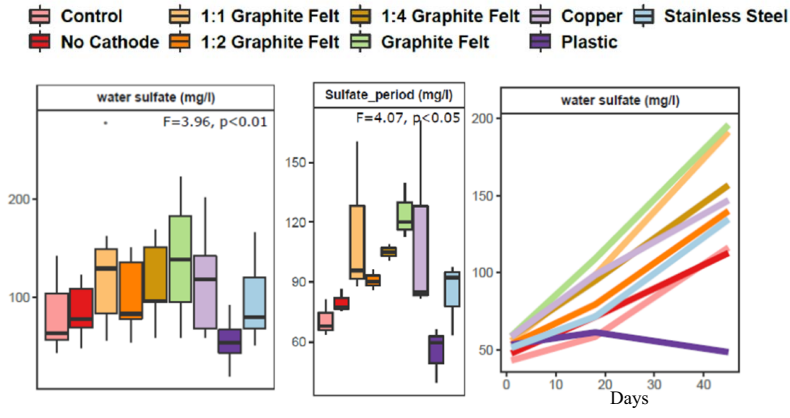

Fig. 11. The box plots display the water concentrations for sulfate, concentrations over the period of experiment and temporal dynamics respectively.

MESR was run without adding any organic carbon to assess NO_3^- reduction in the absence of it. The increase in total organic carbon (TOC) concentration was observed during the cycles with high current density, indicating the growth of microorganisms. However, the increase stopped at 110 mg C-TOC/L in all three reactors. The rise in TOC was rapid, increasing from 10 to 110 mg C-TOC/L in 2–3 days during cycle (3:1). TOC remained around 6 mg C-TOC/L during cycle (2:1), where no NO_3^- reduction was observed (Fig. 12). Although an increase in TOC indicates the presence and growth of microorganisms, it does not necessarily mean that NO_3^- reduction is occurring in the consortium.

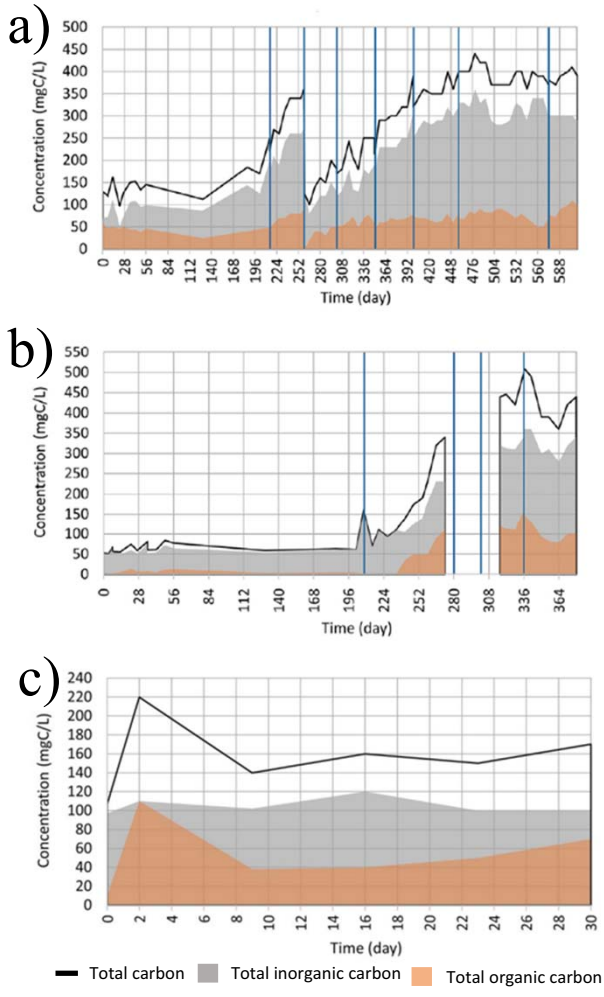

Fig. 12. Temporal dynamics of the TC, TOC and TIC carbon concentrations in single chambered MESR a) Reactor I, b) Reactor II and c) Reactor III (Article II).

3.3 Microbial analysis of MESR

3.3.1 Role and dynamics of N transforming genes in MES

There were significant differences in the abundance of archaea between treatments, but not for bacteria. The proportion of bacteria and archaea in prokaryotic communities was not significantly different between treatments. The abundance of bacterial 16S rRNA genes was higher than that of archaeal 16S rRNA genes in sediment samples. The use of 1:1 graphite felt resulted in decreased gene abundances of both bacteria and archaea, but this trend was not observed in the target gene proportions of the prokaryotic communities (Fig. 13). The temporal dynamics of bacterial 16S rRNA gene parameters showed a decreasing trend, while the archaeal 16S rRNA gene parameters showed an increasing trend, except for the control. Several functional genes were detected in all sediment samples, but their abundances varied between treatments. The archaeal *amoA (amoA arc)* gene abundance was higher than the bacterial *amoA* (*amoA bac)* abundance. The abundances varied in this order *nirS*>*nirK*>*nosZII*>*nosZI*>ANAMMOX-specific 16S rRNA> *amoA arc*>*amoA bac*>*nrfA* (Fig. 14).

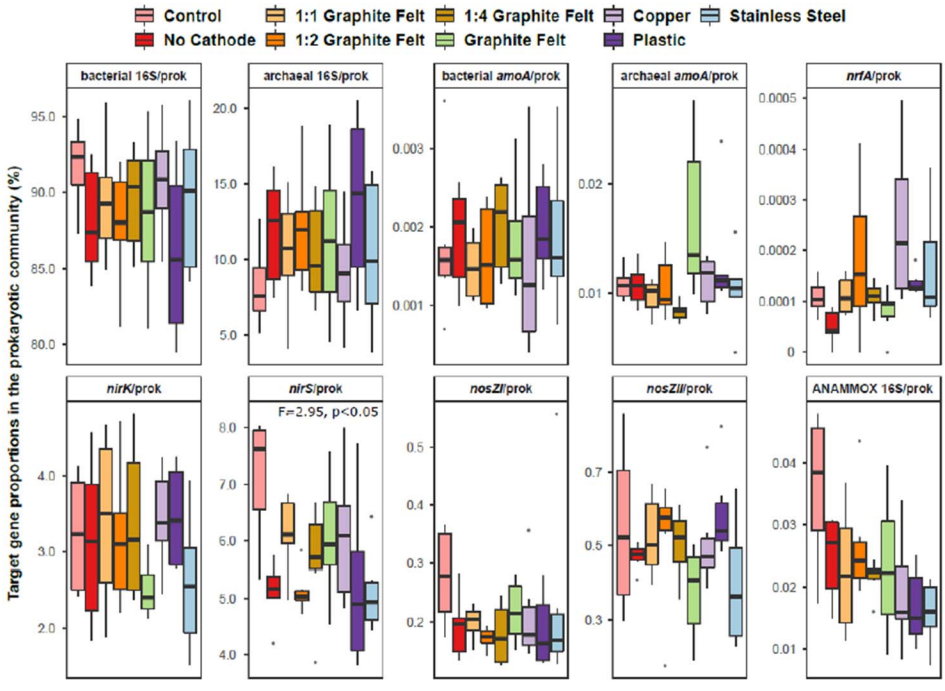

Fig. 13. Box plots of target gene copy numbers proportion in the prokaryotic community (Article I).

The *nirS* proportions in the prokaryotic communities also differed significantly. The controls had higher total abundance for most functional genes except *nrfA* genes, which were either the same or higher in treatments with electrochemical manipulation. Denitrification genes showed lower abundance in treatments with Graphite Felt.

ANAMMOX-specific 16S rRNA gene abundance and proportion in the prokaryotic community decreased in treatments with electrochemical manipulation (Figs. 13, 15). Temporal trends in the different functional genes were similar across treatments, with an increase observed in copy numbers and proportions of *nir*, *nosZI*, *nrfA*, and archaeal *amoA* genes, and a decrease in *nosZII* genes. ANAMMOX-specific 16S rRNA gene showed a substantial decline throughout the experiment. Opposite trends were observed in bacterial *amoA* gene parameters in treatments with graphite felt cathode, while *nirK* genes appeared to be inhibited.

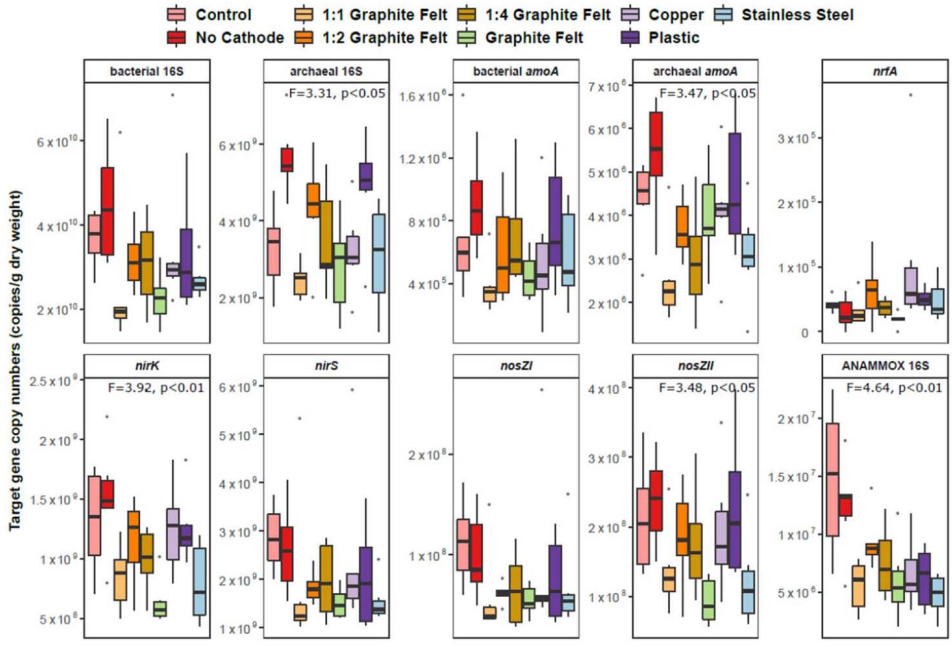

Fig. 14. The box plots represent the target gene copy abundances in varying treatments (Article I).

Archaeal *amoA* genes dominated over bacterial *amoA* genes in MES, possibly due to the engineered conditions of MES. Nitrification was suppressed in cathode treatments, where archaeal *amoA*-possessing microbes were more abundant in control treatments. The abundance of *nir* was higher than *nosZ* in CW-MES systems, and different treatments significantly affected the abundances of *nirS*, *nirK*, and *nosZII*-type denitrifiers. *nirS* and *nosZII* were more abundant in the prokaryotic community than *nirK* and *nosZI*.

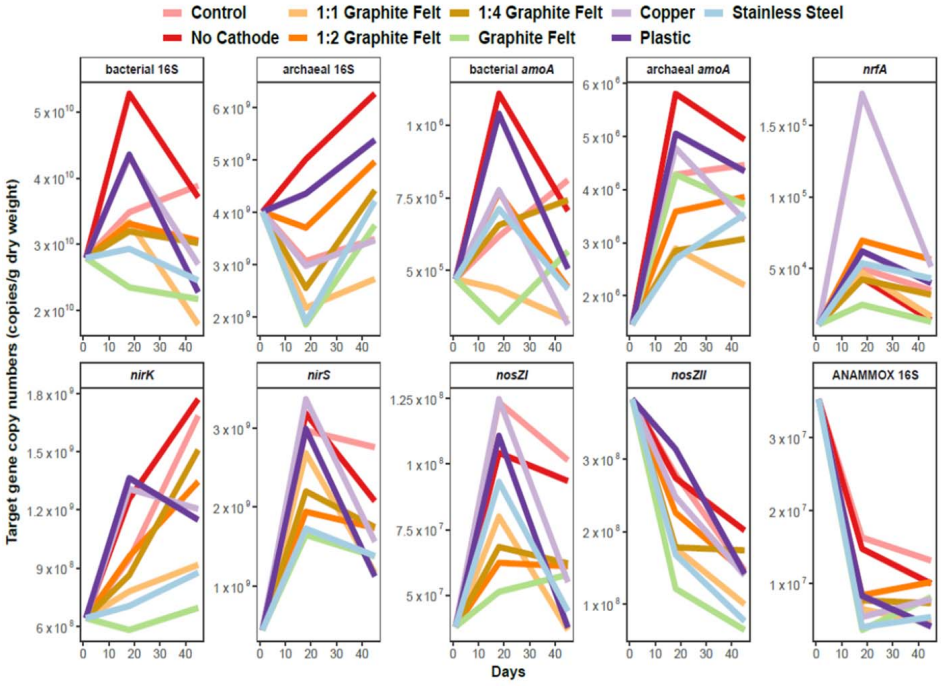

Fig. 15. Temporal dynamics of different gene abundances during the experiment (Article I).

Temporal dynamics of *nirS* and *nosZI* were similar, while those of *nirK* and nosZII were opposite, likely due to the higher frequency of co-occurrence of *nosZ* with *nirS* than with *nirK*. Treatments with cathodes had lower abundance of denitrification genes than controls, suggesting a similar community shift trend as observed with bacteria (Fig. 15).

3.3.2 The share of heterotrophic microbes in MESR electrolyte

It was expected that the number of heterotrophic microorganisms expressed as CFU per 1 mL of electrolyte would increase during the cycle, but no constant increase was observed. Therefore, the TOC rise by 40 mg C-TOC/L, can be most likely due to the proliferation of autotrophic denitrifiers in the electrolyte. There was no correlation between detected bacterial numbers (CFU/mL) and TOC concentration. The abundance of heterotrophic denitrifying bacteria followed a similar pattern, and only a small percentage (1–5%) of cultivated heterotrophs were heterotrophic denitrifying bacteria (Fig. 16). These results suggest that the effective denitrification process is mostly taking place by autotrophic denitrifiers that are unable to grow in the test media. The stable denitrifying community is expected to reside attached to the working electrode of Reactor 1 based on the trends and replicability of other measurements.

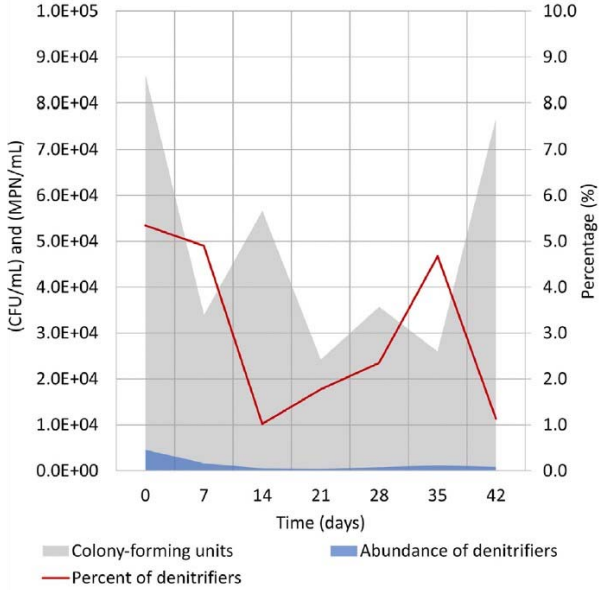

Fig. 16. Heterotrophic culturable microorganisms were enumerated by CFU/mL on nutrient agar, and heterotrophic denitrifying bacteria numbers were evaluated by MPN/mL in Hiltay medium (Article II).

3.3.3 Role and dynamics of N transforming genes in electrode biofilm of MESR

Bacterial and archaeal 16S rRNA, COMAMMOX *amoA, nirS, nirK,* and *nosZI* gene abundances were measured. Bacterial 16S rRNA gene abundance was highest in the CE and WE of set 1, with a smaller difference between three-electrode sets on CEs indicating time has a smaller impact on microbial growth. Archaeal 16S rRNA gene abundance followed the trend resulting in higher gene abundances in set 1. Higher abundances of nitrogen cycle-related genes were detected on electrodes with set 2 but did not exhibit significant NO_3^- reduction after 30 days in the control reactor (Figs. 17a).

Compared to other electrodes, WE (set 3) from cycle (3:1) showed significantly low copy numbers of the *nirS* gene, which may have been the reason why NO_3^- reduction did not occur (Figs. 17b). The presence of the *nirS* and *nosZI* genes on the WE indicate the presence of complete denitrifiers. The abundances of *amoA* and COMAMMOX *amoA* genes were higher on the CE, as expected due to the need for electron acceptors during ammonia oxidation.

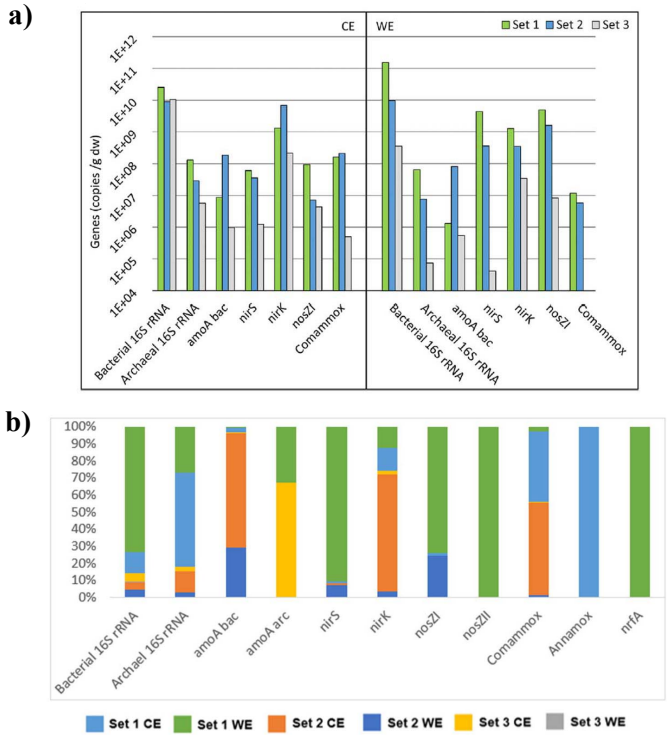

Fig. 17. a) Gene abundances of electrode sets 1–3 on a logarithmic scale. Counter electrode data are shown in the CE section, and working electrode data are shown in the WE section (Article II). b) The stacked bar plot displays the proportion of genes in three sets of electrodes.

3.3.4 Microbial community structure in BES

The microbial community structure in NO_3^--removing BES is dominated by Proteobacteria, followed by *Firmicutes* and *Bacteroidetes*. Many N-transforming bacterial communities belong to the *Proteobacteria* phylum. The biocathode is populated by species including *Thiobacillus, Nitratireductor*, *Shinella, Dyella, Paracoccus, Simplicispira, Geobacter, Thauera, Thermomonas, Azoarcus, Ottowia Nitrospira, Denitratisoma, Dechloromonas,* and *Candidatus Competibacter*. Bioanodes are mainly populated by *Pseudomonas, Curtobacterium*, and *Aeromonas* species (Fig.18).

Denitrification genes such as *narG, napAB, norAC, nirS, nirK, nosZI*, and *nosZII* are enhanced in BES treating NO_3^- rich water. The *nrfA* gene responsible for the DNRA process is significantly enhanced in BES systems. The significant enhancement of *nirS* and *nosZI* genes indicates the presence of autotrophic denitrifiers in BES. The prevalence of the ANAMMOX process in these systems is shown by *hzsB* and ANAMMOX-specific 16S rRNA genes. Ammonia oxidizing genes such as *amoA* and COMAMMOX *amoA* genes were found in higher numbers on the anode or the counter electrode, indicating that the anode is responsible for electron donation or oxidation.

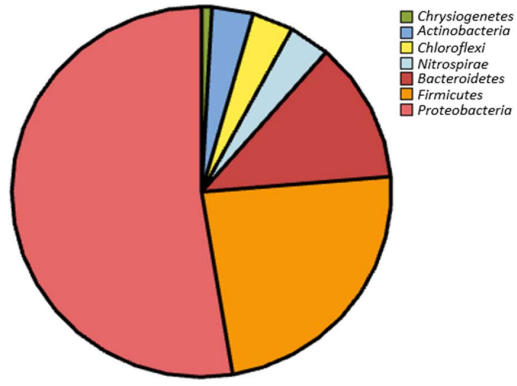

Fig. 18. Proportion of phyla observed in BES utilized for NO_3^- removal (Article III).

3.4 Influence of operational parameters on NO_3^- removal efficiencies

Batch mode is practical for monitoring substrates in BES, but fed-batch and continuous modes are also used for functional and commercial reasons. Continuous mode is the most studied and has the highest NO_3^- removal rates, followed by fed-batch and batch modes. Reactor volume does not significantly affect NO_3^- removal efficiency. Inoculation with denitrifying microbes leads to the highest removal rates in BES, but there are no significant differences among types of inocula. Two-chambered BES have the highest NO_3^- removal rates, but there are no significant differences among the number of chambers for removal rates (Fig. 19).

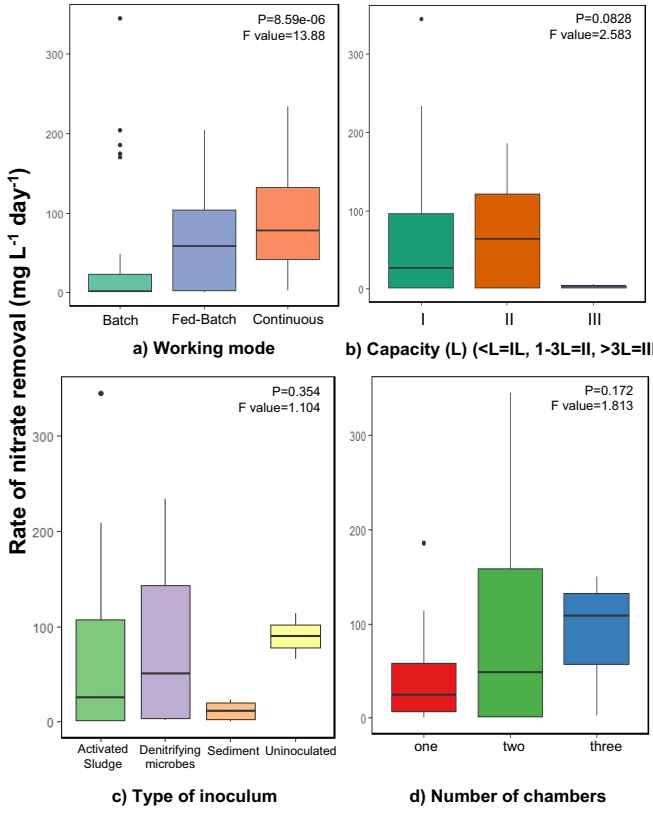

Fig. 19. The boxplots display operational parameters working mode (a), capacity (b), type of inoculum (c), and the number of chambers (d) compared to the NO_3^- removal rate (Article III).

The mode of operation of the BES determines nutrient and cofactor concentrations. Inoculum influences the microbial community in the BES and acts as a starter culture. Denitrifying sludge may enhance bio-cathode activity. The microbial community structure in BES with biocathodes differs from those without. Chambers and cation exchange membranes help maintain pH. Two-chamber systems with granular carbon and carbon paper could offer optimal removal efficiencies. Wastewater characteristics play a crucial role in determining the microbial community structure. BES capacity does not significantly affect removal efficiencies, and system scalability can be achieved by focusing on other design and operational parameters. The relative importance of various parameters can be determined by observing changes in removal efficiencies and analyzing the features selected in (Table C).

3.5 Feature selection using random forest algorithm to determine the importance of parameters on NO_3^- removal rates

Feature selection using a random forest classification algorithm was conducted to determine the significance of different factors on the rate of NO_3^- removal and percentage removal. For the rate of removal, all the components and operational parameters were found to be important, while the inoculum was tentatively identified as important after model adjustments. However, for the percentage removal, the number of chambers was deemed unimportant. The random forest classification analysis for the percentage of removal revealed that electrode materials, working mode, inoculum type, and capacity were considered important factors. These findings indicate the varying degrees of importance of different factors in the NO_3^- removal process (Fig. 20).

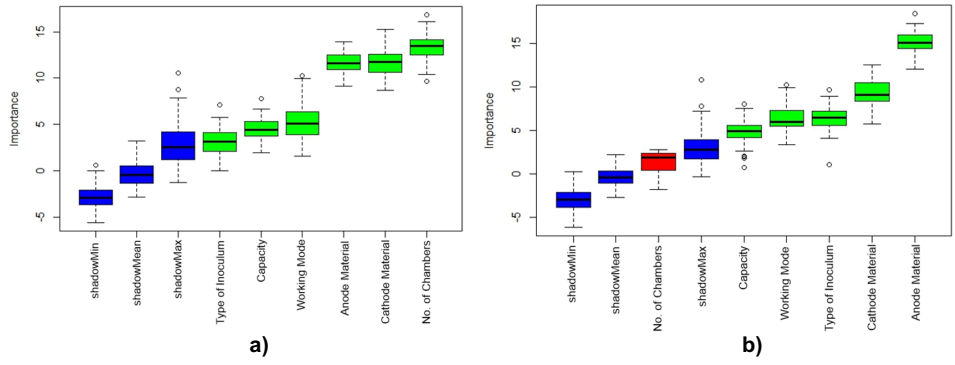

Fig. 20. Feature selection using random forest classifier of various factors on their rate of NO_3^- removal (mg $liter^{-1}$ day^{-1}) (a) and NO_3^- removal percentage (%) (b) (Article III).

3.6 Sustainability of the MES investigated by estimating N_2O fluxes

N_2O emission values directly before soil sampling showed no statistical differences between treatments ($p > 0.05$), but highest emissions were observed for treatments with cathodes 1:1 graphite felt, copper, plastic, and stainless steel (Fig. 21). The smaller the size of cathode, lower N_2O fluxes were registered.

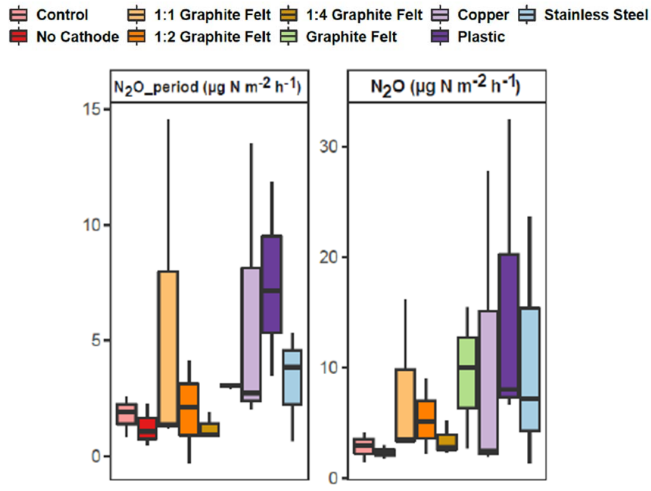

Fig. 21. The box plots display the N_2O fluxes over the period and the NO_2^- fluxes observed in varying treatments respectively (Article I).

3.7 Electrochemistry: Cyclic voltammetry measurement of MES and MESR

Cyclic voltammetry was conducted on cathode reactor samples and two out of three replicates with graphite felt cathodes showed a reduction system, indicated by a reduction peak at around −0.3 V vs. Ag/AgCl under helium saturation before NO_3^- addition (Fig. 22).

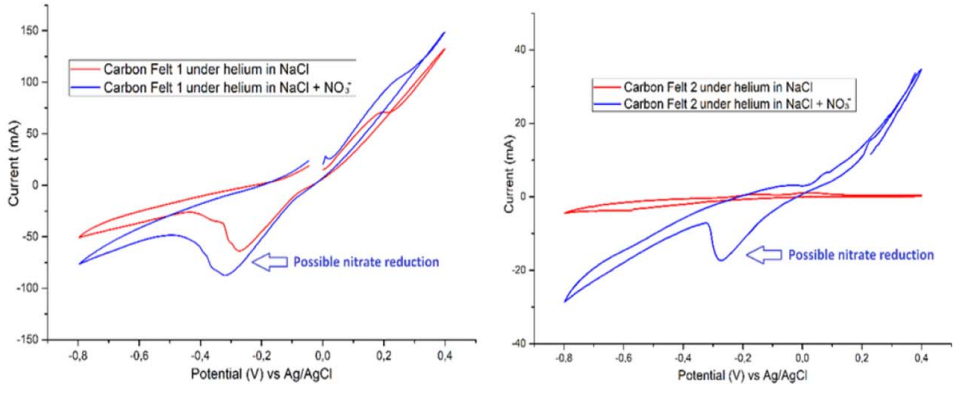

Fig. 22. Cyclic voltammograms of carbon felt before and after $NaNO_3^-$ addition under He saturation (Article I).

The peak current of this system increased after NO_3^- addition. The other cathode materials did not show similar reduction peaks. The average polarizations of the cathode electrodes were: +0.136 V vs. SHE for carbon felt, −0.02 V vs. SHE for copper, and −0.166 V vs. SHE for stainless steel electrodes. The average polarizations of the anode electrodes were: −0.03 V vs. SHE for carbon felt, −0.08 V vs. SHE for copper, and −228 V vs. SHE for stainless steel electrodes.

Cyclic voltammetry (CV) measurements were conducted throughout the experiment to track changes on the working electrodes (WEs). The measurements presented in Fig. 22 were taken at different time points, with different colored dots indicating each time point. The CV was conducted using a quick potential sweep rate of 10 mV/s to minimize harm to microorganisms. On day 7, a reduction peak of around −300 mV appeared, which is consistent with previous studies on autotrophic denitrification. After lowering the WE potential to −756 mV, the CV measurements were taken in a smaller potential range to prevent harm to microorganisms, and a potential sweep rate of 0.25 mV/s was used. The overall current density increased over time, and at lower potentials, the increase in current density was more significant. The WE capacitance increased significantly over time, likely due to changes in WE structure and biofilm growth. The CV measurements suggest that the *T. denitrificans* biofilm surface area continued to expand, even at higher potentials.

3.8 Relationships between target genes, physicochemical parameters and N_2O flux

The analysis found significant correlations between target genes and environmental factors in most treatments (except control and no cathode), with positive correlations between sediment DC/DN and various bacterial genes and negative correlations with *nirK* and ANAMMOX-specific genes. Sediment DOC was related to bacterial and ANAMMOX-specific genes. Water NO_3^- was positively correlated with *amoA arc* but negatively with archaeal 16S rRNA and *nirK*. Water NO_3^- was positively correlated with *nirS* but negatively with *nosZII* and ANAMMOX-specific genes. Water sulfate had negative correlations with *nosZII* and *nrfA* genes. Additional significant relationships were found but not confirmed by Benjamini-Hochberg correction. *nrfA* abundance was positively correlated with N_2O emissions, while the proportion of *nosZI* was positively correlated with one-time N_2O measurements but negatively correlated with average N_2O emissions (Fig. 23).

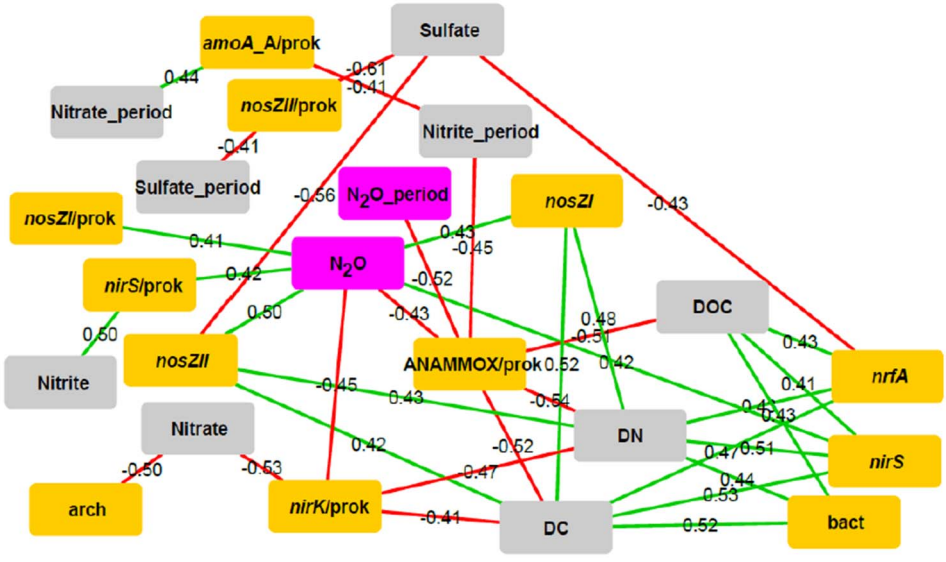

Fig. 23. The Benjamini-Hochberg corrected Spearman correlation network ($p < 0.05$) for each target gene parameter and environmental factors (Article I).

4. DISCUSSION

The research encompassed in this thesis aim at understanding the microbial and environmental factors affecting NO_3^- removal. Although many regions in Asia, Europe, and Africa have detected NO_3^- concentrations in groundwater that surpass WHO recommendations (Abascal et al., 2022), it is concerning that an estimated 60% of rural areas in Asia and Africa depend on groundwater for their drinking water (Margat and van der Gun et al., 2013). The groundwater, NO_3^- contaminated water from the industries have high concentration of NO_3^-, whereas the presence of excessive NO_3^- levels in surface water can lead to eutrophication, resulting in a decline in biodiversity, as per the findings of Camargo and Alonso et al., (2006). Consequently, it is crucial to explore and implement diverse technologies that can effectively eliminate NO_3^- from water. MES provide a contained space for removal of NO_3^- and the specific conditions devoid of oxygen to carry out complete denitrification. The efficiencies of this systems displayed high removal rates in non-conductive treatments and controls i.e. plastic electrode, no cathode and no electrodes respectively. The short-circuit provides continuous supply of electrons and therefore fulfills the need of electrons for the reduction processes to occur. Microbial community structure has seen to be drastically affected by the electrochemical manipulation, eventually leading to affect microbial activity and curb NO_3^- removal rates (Aracic et al., 2014). Though there aren't any significant difference observed in removal efficiencies among varying cathode materials and size, there was an interesting observation of the N_2O flux declining with the size of the cathode observed i.e. smaller the cathode size, the less were the N_2O emissions detected. The denitrification genes i.e. *nirS, nirK, nosZI, nosZII* and ANAMMOX 16S are in abundances in the order of the declining size of the cathode, therefore the reduction in N_2O emissions could be attributed to the incomplete denitrification in these treatments. The primary cause of N_2O emissions in MES appears to be linked to *nirS*-type denitrifiers, although there are some indications that microbes carrying DNRA may also have a significant contribution to N_2O production. DNRA activity as previously observed in electrochemical systems (Su et al., 2022). Although the electroactive potential and traits of the ANAMMOX bacteria, specifically the *Candidatus Brocadia sinica* and *Candidatus Scalindua sp.* varieties, have been poorly researched, these microorganisms still possess significant interest (Logan et al., 2019). The ANAMMOX processes in MES is highly curbed, this might be due to the less NO_2^- concentrations in the systems. Two graphite felt cathodes exhibited an electrochemical reaction when NO_3^- was added at 0.3 V. This observation indicates that the biofilm on these cathodes may contain electroactive denitrifying microorganisms. Archaea have a widespread presence in diverse environments and possess unique traits (Moissl-Eichinger et al., 2018). It is probable that they exhibit a considerable degree of resistance towards electrochemical manipulation, or that such manipulation might have the potential to boost the abundance of archaea. The electrochemical manipulation appeared to have minimal impact on the microorganisms conducting DNRA in our MES systems, and some treatments even resulted in

higher levels and proportions of DNRA microbes in comparison to the controls. The increase in *nrfA* gene copy numbers could be due to the diverse metabolic pathways of DNRA microbes that enable them to flourish in various environments (Song et al., 2014). DNRA microorganisms maintain the N levels in the system by converting NO_2^- into NH_4^+, which influenced the increase in *amoA*-harbouring microbes. Our study revealed that there is competition for essential nutrients, as suggested by the relationships between gene parameters and sediment DC, DOC, DN, as well as water NO_3^- and NO_2^- concentrations. Denitrification and ANAMMOX exhibited the strongest competition, while the impact of nitrification was negligible. Additionally, water sulfate content inhibited the abundance of major N-cycle genes.

The MESR showed significant removal rates utilizing *Thiobacillus denitrificans* as an inoculum. It can carry out autotrophic denitrification using inorganic compounds as electron donors and inorganic carbon sources for growth. However, a low concentration of electron donors can hinder NO_3^- removal from water. Microbial electrosynthesis substitutes the microorganisms' demand for electron donors, with electrons provided via the electrode.

The NO_3^- concentration was increased approximately by half for Reactors 1 and 2 in an attempt to initiate the active proliferation of denitrifying microorganisms, the concentrations that initiated the activity were 82.4 and 70.8 mg $N\text{-}NO_3^-/L$ respectively.

The reduction of NO_3^- in MESR was driven by the applied current, and the pH remained stable in both reactors which was achieved by using CE with 3.6 times higher surface area compared to the WE. The higher surface imparts lower O_2 concentration in the MESR i.e. The DO was in the range of 0.3–0.5 mg O_2/L, but it was still in the range to allow autotrophic denitrification (Gómez et al., 2002; Qambrani and Oh et al., 2013). The potential at which NO_3^- removal was initiated was −756mV. Usually, accumulation of NO_2^- as an intermediate is observed during the autotrophic denitrification if the system is not functioning optimally, which wasn't the case with BES (Al-Mamun and Baawain et al., 2015; Li et al., 2017). However, reduction down to NH_4^+ was not anticipated. The DNRA can cause NO_3^- reduction to NH_4^+ and compete with autotrophic denitrification in the current system. The presence of *nrfA* gene abundances on the WE of the reactor 1 can confirm the presence of microbes possessing abilities to carry out DNRA. *Pseudomonas alcaliphila* strain MBR can undergo both denitrification and DNRA when an electrode is used as the sole electron donor in a double chamber bio-electrochemical system (BES) (Su et al., 2022). DNRA can still occur with a WE potential as low as −303 mV. However, in our experimental setup, the NH_4^+ concentration did not exceed the WE potential of −556 mV. The pH of the system was slightly affected by the presence of NH_4^+. Our findings additionally support the notion that the autotrophic denitrifying community likely remains consistent and is not substituted by heterotrophs throughout the cycle. Considering the patterns observed in other measurements, it is anticipated that the stable denitrifying community is located on the electrode surface of BES. The

transition of the microbial community from heterotrophic to autotrophic denitrification is possible, although it requires specific conditions and is considered a laborious process (Huang et al., 2022). The WE (set 3) in cycle (3:1) demonstrated significantly lower copy numbers of the *nirS* gene compared to another electrode sets. The *nirS* gene is responsible for the second step of denitrification, which involves the conversion of NO_2^- to NO (Lam and Kuypers et al., 2011). These low gene abundances could explain the absence of NO_3^- reduction in abiotic reactor. Moreover, the abundances of archaeal 16S rRNA genes and the *commamox* community were found to be extremely low on this particular electrode.

The counter electrode (CE) demonstrated elevated quantities of *amoA* and COMAMMOX *amoA* genes associated with NH_3 oxidation (Lam and Kuypers et al., 2011). This outcome is in line with expectations, as the CE can function as an electron acceptor during the oxidation process. The co-occurrence of the *nirS* and *nosZ* genes is more abundant in denitrifiers compared to the *nirK* gene (Hallin et al., 2018). Our results indicate similar abundances of nirS and *nosZI* genes on the working electrode (WE), suggesting the presence of complete denitrifiers. The abundance of *nosZI* on WE over CE also suggests the involvement of *nosZI* harbouring denitrifiers. We observed complete denitrifies exhibit resilience towards electrochemical manipulation. *nirK* gene harbouring microbes are fairly higher in abundances in nature (Hallin et al., 2018, Lam and Kuypers et al., 2011). On day 7, the reduction peak of around −300 mV was observed which was registered in several studies of BES focusing on autotrophic denitrification (Kondaveeti and Min et al., 2013; Pous et al., 2014; Yu et al., 2015; Zhou et al., 2016; Ceballos-Escalera et al., 2021). The increase in capacitance and improved wetting of the graphite felt over time may be due to the expanded surface area of the working electrode (WE) in contact with water and the growth of the biofilm, leading to enhanced bacterial activity. An initial WE potential of at least −756 mV was necessary to initiate the NO_3^- reduction process, which remained effective even at lower potentials. Cyclic voltammetry (CV) measurements indicated continuous expansion of the *T. denitrificans* biofilm surface area, as evidenced by the increasing WE current density |j| during cycles with higher potentials. There was a rise in TOC with the rise in current density, and can be therefore attributed to the growth of microbes on the WE. The heterotrotrophic denitrifying bacteria were just a fraction of the enumerated heterotrophic microbes therefore, suggesting that the biofilm consists of community successfully carrying out autotrophic denitrification.

A larger surface area by ~12.5 cm^2/L has displayed ~57% increase in NO_3^- removal rates, the higher surface area was imparted by graphite felt in MESR, while previously studied Pous et al., 2016 utilized graphite rod. The appropriate choice of electrode material therefore, largely influences the NO_3^- removal efficiencies, the choice of electrode material remains carbon in majority of the studies with granular carbon and carbon paper displaying the highest removal efficiencies compared to other cathode and anode materials studied so far for applications of BES for NO_3^- removal respectively. Higher surface area imparted by these materials aid in higher microbial abundance and therefore, directly impacts

the BES efficiency. Working electrodes have been displayed to inhabit the N-transforming microbial communities, which aids in the enhancement of the reduction process, whereas the strengthening of cathode leads in enhanced electron transfer (Wang et al., 2021). Biocathodes can employ various processes for NO_3^- removal in comparison to abiotic cathodes (Al-Mamun et al., 2017). The operational mode of BES impacts nutrient concentrations and cofactor availability. Inoculation affects the microbial community structure and acts as a starter culture. Denitrifying sludge enhances bio-cathode activity. Biocathode-based systems undergo substantial shifts in microbial community structure, with the electrode housing microorganisms that catalyze cathodic reactions (Liu et al., 2014). Chambers with cation exchange membranes maintain pH (Fig. 24a). The microbial community structure largely depends on the water treated in the BES, as observed in our studied single chambered BES and MES, higher NO_3^- concentrations triggered NO_3^- removal in single chambered BES. As different enzymes have varying affinities and feedbacks, the C/N ratio governs biological N elimination processes (Bonassa et al., 2021). The C/N ratio in the system is a key factor in autotrophic denitrification; when the C/N ratio rises, NO_2^- buildup increases and autotrophic denitrification in BES falls (Van Doan et al., 2013). NO_3^- concentration causes accelerated autotrophic denitrification. As a result, BES can effectively treat high NO_3^- effluents with low carbon content (Pous et al., 2014). The C/N ratio has no discernible effect on the anode transforming efficiency (Huang et al., 2013). When used for NO_3^- treatment, autotrophic denitrification yields removal efficiencies comparable to that of traditional systems (Chen et al., 2021). A high C/N ratio inhibits the ANAMMOX process; specifically, 5.8 g COD/N promotes nitration while 3.5 g COD/N supports the process (Bonassa et al., 2021). After external stimulation of 1.5V, it has been seen that marine ANAMMOX bacteria are boosted (Hu et al., 2022). Ex-situ N^{15} tracer tests demonstrated that BES supported heterotrophic denitrification and the ANAMMOX process for the removal of NO_3^- (Koffi et al., 2021).

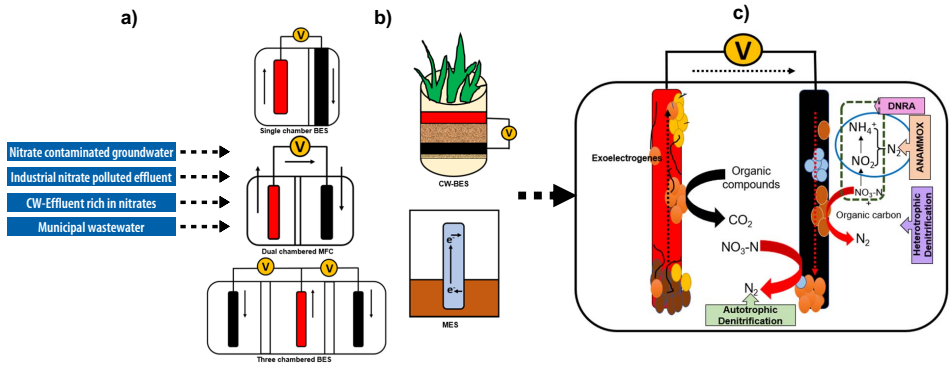

Fig. 24. a) Sources of NO_3^--contaminated water, b) Types of Bio-electrochemical systems (BES), c) Schematic diagram of the processes of NO_3^- transformation in BES. (red electrode represents-anode, black electrode represents-cathode) (Article III).

BES enhanced DNRA process which can be employed to recover N, and the recovered NH_4^+ can be utilized as fertilizer, whereas BES also has the capacity to completely remove NO_3^- (Li et al., 2022; Zhao et al., 2023). It has been demonstrated that the DNRA process loses its ability to produce electrons when C/N=6 (Liang et al., 2021) therefore, the process is supported by low carbon- high NO_3^- concentration. The feature selection results in contradictory results for different units of NO_3^- removal efficiencies, therefore it's essential to have a common and standardized unit of referring to NO_3^- removal rates, for better access and evolution of BES in treating NO_3^-. Different BES can be employed for varying purposes e.g. When agricultural run-off is high in volume constructed wetland conjugated with BES can be employed as CW reduces the carbon load of the run-off (Kill et al., 2018) and high NO_3^- effluent can be further processed by BES. MFC can be employed at defined volumes of point sources of NO_3^- effluent from the industries, whereas MES displays high potential for scalability due to its simpler design (Fig. 24).

5. CONCLUSIONS

MES displayed efficient NO_3^- and NO_2^- removal. The archaeal nitrifying community showed higher resilience towards electrochemical manipulation. The *nirK* type of denitrifiers were significantly affected in MES, although the presence of *nirS* and *nosZI* type denitrifiers would be attributed for production and consumption of N_2O flux in MES. The smaller the cathode, lower where the N_2O flux and consequently higher abundances of denitrifying genes therefore, asserting the influence of short circuit on the N-transforming communities. The decline in TOC is correlated to the decrease in gene abundances, therefore the majorly involved processes in MES responsible for NO_3^- removal would be heterotrophic denitrification, though relatively less in proportion ANAMMOX 16S genes were observed in MES. DNRA activity is largely supported by electrochemical manipulation, *nrfA* gene displayed a significant rise in MES and would be responsible for the generation of N_2O fluxes.

MESR provides a stable reduction of NO_3^-, the WE were effectively run at carbon-deficient conditions and still shows stable removal efficiencies by *Thiobacillus denitrificans* as an inoculum. The NO_3^- removal was initiated at −756 mV, triggered after higher NO_3^- concentrations. At, −656 mV potential, the MESR achieved its optimum performance, exhibiting a remarkable Faradaic efficiency of 71%. A significant portion of the applied electrical current was utilized for the desired NO_3^- reduction process. Additionally, the system demonstrated an impressive NO_3^- removal rate of 3.8 ± 1.2 mg N-NO_3^- $L^{-1}day^{-1}$). The presence of heterotrophic denitrifiers was <5% in MESR therefore, indicative of autotrophic denitrification. The abundance of *nirS* and *nosZI* genes was significantly higher on WE compared to CE indicating that the predominantly driven process was autotrophic denitrification. The conversion of NO_3^- to NH_4^+ was observed which can be credited to the abundances of *nrfA* genes detected only on WE. BES is a powerful system for treating NO_3^- contaminated water, enhancing denitrification and N-transforming processes. The choice of electrode material and surface area influences NO_3^- removal efficiency, with granular carbon and carbon paper showing better performance as cathode and anode respectively. The water composition determines microbial communities in BES. System volume has minimal impact on NO_3^- removal efficiency, assuring scalability of the BES. Operational mode and chamber design affect nutrient availability and pH maintenance. Standardized units for NO_3^- removal rate, are necessary for thorough understanding of the BES efficiency. External power supply (e.g., MESR) accelerates NO_3^- reduction with higher removal rates than MFC. Our analysis suggests a continuous two-chamber BES with granular carbon or carbon paper as electrodes and denitrifying microbes as inoculum for optimal NO_3^- removal efficiency.

REFERENCES

Abascal, E., Gómez-Coma, L., Ortiz, I., Ortiz, A., 2022. Global diagnosis of nitrate pollution in groundwater and review of removal technologies. Science of The Total Environment 810, 152233. https://doi.org/10.1016/j.scitotenv.2021.152233

Al-Mamun, A., Baawain, M.S., 2015. Accumulation of intermediate denitrifying compounds inhibiting biological denitrification on cathode in Microbial Fuel Cell. J. Environmental Health Science and Engineering 13, 81. https://doi.org/10.1186/s40201-015-0236-5

Al-Mamun, A., Baawain, M.S., Egger, F., Al-Muhtaseb, A.H., Ng, H.Y., 2017. Optimization of a baffled-reactor microbial fuel cell using autotrophic denitrifying bio-cathode for removing nitrogen and recovering electrical energy. Biochemical Engineering Journal 120, 93–102. https://doi.org/10.1016/j.bej.2016.12.015

Amanze, C., Anaman, R., Wu, Xiaoyan, Alhassan, S.I., Yang, K., Fosua, B.A., Yunhui, T., Yu, R., Wu, Xueling, Shen, L., Dolgor, E., Zeng, W., 2023. Heterotrophic anodic denitrification coupled with cathodic metals recovery from on-site smelting wastewater with a bioelectrochemical system inoculated with mixed Castellaniella species. Water Research 231, 119655. https://doi.org/10.1016/j.watres.2023.119655

Aracic, S., Semenec, L., Franks, A.E., 2014. Investigating microbial activities of electrode-associated microorganisms in real-time. Frontiers in Microbiology 5, 663. https://doi.org/10.3389/fmicb.2014.00663

Arp, D.J., Stein, L.Y., 2003. Metabolism of Inorganic N Compounds by Ammonia-Oxidizing Bacteria. Critical Reviews in Biochemistry and Molecular Biology 38, 471–495. https://doi.org/10.1080/10409230390267446

Bernhard, A 2010. The Nitrogen Cycle: Processes, Players, and Human Nature news. https://www.nature.com/scitable/knowledge/library/the-nitrogen-cycle-processes-players-and-human-15644632.

Bonassa, G., Bolsan, A.C., Hollas, C.E., Venturin, B., Candido, D., Chini, A., De Prá, M.C., Antes, F.G., Campos, J.L., Kunz, A., 2021. Organic carbon bioavailability: Is it a good driver to choose the best biological nitrogen removal process? Science of The Total Environment 786, 147390. https://doi.org/10.1016/j.scitotenv.2021.147390

Camargo, J.A., Alonso, Á., 2006. Ecological and toxicological effects of inorganic nitrogen pollution in aquatic ecosystems: A global assessment. Environment International 32, 831–849. https://doi.org/10.1016/j.envint.2006.05.002

Campeciño, J., Lagishetty, S., Wawrzak, Z., Sosa Alfaro, V., Lehnert, N., Reguera, G., Hu, J., Hegg, E.L., 2020. Cytochrome c nitrite reductase from the bacterium Geobacter lovleyi represents a new NrfA subclass. Journal of Biological Chemistry 295, 11455–11465. https://doi.org/10.1074/jbc.RA120.013981

Ceballos-Escalera, A., Pous, N., Chiluiza-Ramos, P., Korth, B., Harnisch, F., Bañeras, L., Balaguer, M.D., Puig, S., 2021. Electro-bioremediation of nitrate and arsenite polluted groundwater. Water Research 190, 116748. https://doi.org/10.1016/j.watres.2020.116748

Cecconet, D., Devecseri, M., Callegari, A., Capodaglio, A.G., 2018. Effects of process operating conditions on the autotrophic denitrification of nitrate-contaminated groundwater using bioelectrochemical systems. Science of The Total Environment 613–614, 663–671. https://doi.org/10.1016/j.scitotenv.2017.09.149

Clauwaert, P., Rabaey, K., Aelterman, P., De Schamphelaire, L., Pham, T.H., Boeckx, P., Boon, N., Verstraete, W., 2007. Biological Denitrification in Microbial Fuel Cells. Environmental Science and Technology. 41, 3354–3360. https://doi.org/10.1021/es062580r

Chen, D., Wei, L., Zou, Z., Yang, K., Wang, H., 2016. Bacterial communities in a novel three-dimensional bioelectrochemical denitrification system: the effects of pH. Applied Microbiology and Biotechnology 100, 6805–6813. https://doi.org/10.1007/s00253-016-7499-3

Chen, D., Wang, H., Yang, K., Ma, F., 2018. Performance and microbial communities in a combined bioelectrochemical and sulfur autotrophic denitrification system at low temperature. Chemosphere 193, 337–342. https://doi.org/10.1016/j.chemosphere.2017.11.017

Chen, D., Yang, L., Li, Z., Xiao, Z., 2021. Application of humin-immobilized biocathode in a continuous-flow bioelectrochemical system for nitrate removal at low temperature. Environmental Research 202, 111677. https://doi.org/10.1016/j.envres.2021.111677

Conners, E.M., Rengasamy, K., Bose, A., 2022. Electroactive biofilms: how microbial electron transfer enables bioelectrochemical applications. Journal of Industrial Microbiology and Biotechnology 49, kuac012. https://doi.org/10.1093/jimb/kuac012

Daims, H., Lücker, S., Paslier, D.L., Wagner, M., 2011. Diversity, Environmental Genomics, and Ecophysiology of Nitrite-Oxidizing Bacteria, in: Nitrification. John Wiley & Sons, Ltd, pp. 295–322. https://doi.org/10.1128/9781555817145.ch12

Di Capua F., Pirozzi F., Lens P. N. L., Esposito G. 2019. Electron donors for autotrophic denitrification. Chemical Engineering. Journal. 362, 922–937. https://doi.org/10.1016/j.cej.2019.01.069

Fang, Y., Wang, H., Han, J., Li, Z., Wang, A., 2022. Enhanced nitrogen removal of constructed wetlands by coupling with the bioelectrochemical system under low temperature: Performance and mechanism. Journal of Cleaner Production 350, 131365. https://doi.org/10.1016/j.jclepro.2022.131365

Fowler, D., Coyle, M., Skiba, U., Sutton, M.A., Cape, J.N., Reis, S., Sheppard, L.J., Jenkins, A., Grizzetti, B., Galloway, J.N., Vitousek, P., Leach, A., Bouwman, A.F., Butterbach-Bahl, K., Dentener, F., Stevenson, D., Amann, M., Voss, M., 2013. The global nitrogen cycle in the twenty-first century. Philosophical Transactions of the Royal Soiety. B 368, 20130164. https://doi.org/10.1098/rstb.2013.0164

Galloway, J.N., Townsend, A.R., Erisman, J.W., Bekunda, M., Cai, Z., Freney, J.R., Martinelli, L.A., Seitzinger, S.P., Sutton, M.A., 2008. Transformation of the Nitrogen Cycle: Recent Trends, Questions, and Potential Solutions. Science 320, 889–892. https://doi.org/10.1126/science.1136674

Gómez, M.A., Hontoria, E., González-López, J., 2002. Effect of dissolved oxygen concentration on nitrate removal from groundwater using a denitrifying submerged filter. Journal of Hazardous Materials 90, 267–278. https://doi.org/10.1016/s0304-3894(01)00353-3

Gregory, K.B., Bond, D.R., Lovley, D.R., 2004. Graphite electrodes as electron donors for anaerobic respiration. Environmental Microbiology 6, 596–604. https://doi.org/10.1111/j.1462-2920.2004.00593.x

Guo, W., Ying, X., Zhao, N., Yu, S., Zhang, X., Feng, H., Zhang, Y., Yu, H., 2023. Interspecies electron transfer between Geobacter and denitrifying bacteria for nitrogen removal in bioelectrochemical system. Chemical Engineering Journal 455, 139821. https://doi.org/10.1016/j.cej.2022.139821

Hallin, S., Philippot, L., Löffler, F.E., Sanford, R.A., Jones, C.M., 2018. Genomics and Ecology of Novel N2O-Reducing Microorganisms. Trends in Microbiology 26, 43–55. https://doi.org/10.1016/j.tim.2017.07.003

Hao, R., Li, S., Li, J., Meng, C., 2013. Denitrification of simulated municipal wastewater treatment plant effluent using a three-dimensional biofilm-electrode reactor: Operating performance and bacterial community. Bioresource Technology 143, 178–186. https://doi.org/10.1016/j.biortech.2013.06.001

Hoareau, M., Erable, B., Bergel, A., 2019. Microbial electrochemical snorkels (MESs): A budding technology for multiple applications. A mini review. Electrochemistry Communications 104, 106473. https://doi.org/10.1016/j.elecom.2019.05.022

Hu, Z., Li, J., Zhang, Y., Liu, W., Wang, A., 2022. Exerting applied voltage promotes microbial activity of marine anammox bacteria for nitrogen removal in saline wastewater treatment. Water Research 215, 118285. https://doi.org/10.1016/j.watres.2022.118285

Huang, B., Feng, H., Wang, M., Li, N., Cong, Y., Shen, D., 2013. The effect of C/N ratio on nitrogen removal in a bioelectrochemical system. Bioresource Technology 132, 91–98. https://doi.org/10.1016/j.biortech.2012.12.192

Huang, X., Duan, C., Yu, J., Dong, W., 2022. Transforming heterotrophic to autotrophic denitrification process: Insights into microbial community, interspecific interaction and nitrogen metabolism. Bioresource Technology 345, 126471. https://doi.org/10.1016/j.biortech.2021.126471

Kill, K., Pärn, J., Lust, R., Mander, Ü., Kasak, K., 2018. Treatment efficiency of diffuse agricultural pollution in a constructed wetland impacted by groundwater seepage, Water 10, 1601. https://doi.org/10.3390/w10111601.

Koffi, N.J., Okabe, S., 2021. Bioelectrochemical anoxic ammonium nitrogen removal by an MFC driven single chamber microbial electrolysis cell. Chemosphere 274, 129715. https://doi.org/10.1016/j.chemosphere.2021.129715

Kondaveeti, S., Min, B., 2013. Nitrate reduction with biotic and abiotic cathodes at various cell voltages in bioelectrochemical denitrification system. Bioprocess Biosystems Engineering 36, 231–238. https://doi.org/10.1007/s00449-012-0779-0

Kondaveeti, S., Lee, S.-H., Park, H.-D., Min, B., 2014. Bacterial communities in a bioelectrochemical denitrification system: The effects of supplemental electron acceptors. Water Research 51, 25–36. https://doi.org/10.1016/j.watres.2013.12.023

Kondaveeti, S., Kang, E., Liu, H., Min, B., 2019. Continuous autotrophic denitrification process for treating ammonium-rich leachate wastewater in bioelectrochemical denitrification system (BEDS). Bioelectrochemistry 130, 107340. https://doi.org/10.1016/j.bioelechem.2019.107340

Kong, Z., Wang, H., Yan, G., Yan, Q., Kim, J.R., 2023. Limited dissolved oxygen facilitated nitrogen removal at biocathode during the hydrogenotrophic denitrification process using bioelectrochemical system. Bioresource Technology 372, 128662. https://doi.org/10.1016/j.biortech.2023.128662

Kursa, M.B., Rudnicki, W.R., 2010. Feature Selection with the Boruta Package. Journal of Statistical Software 36, 1–13. https://doi.org/10.18637/jss.v036.i11

Kuypers, M.M.M., Marchant, H.K., Kartal, B., 2018. The microbial nitrogen-cycling network. Nature Reviews Microbiology 16, 263–276. https://doi.org/10.1038/nrmicro.2018.9

Li, Y., Bali, S., Borg, S., Katzmann, E., Ferguson, S.J., Schüler, D., 2013. Cytochrome cd1 Nitrite Reductase NirS Is Involved in Anaerobic Magnetite Biomineralization in Magnetospirillum gryphiswaldense and Requires NirN for Proper d1 Heme Assembly. Journal of Bacteriology 195, 4297–4309. https://doi.org/10.1128/JB.00686-13

Li, P., Wang, Y., Zuo, J., Wang, R., Zhao, J., Du, Y., et al. 2017. Nitrogen removal and N2O accumulation during hydrogenotrophic denitrification: Influence of environmental factors and microbial community characteristics. Environmental Science & Technology 51, 870–879. doi: 10.1021/acs.est.6b00071

Liu, H., Yan, Q., Shen, W., 2014. Biohydrogen facilitated denitrification at biocathode in bioelectrochemical system (BES). Bioresource Technology 171, 187–192. https://doi.org/10.1016/j.biortech.2014.08.056

Li, J., Li, Y., Chen, P., Sathishkumar, K., Lu, Y., Naraginti, S., Wu, Y., Wu, H., 2022. Biological mediated synthesis of reduced graphene oxide (rGO) as a potential electron shuttle for facilitated biological denitrification: Insight into the electron transfer process. Journal of Environmental Chemical Engineering 10, 108225. https://doi.org/10.1016/j.jece.2022.108225

Liang, D., Li, C., He, W., Li, Z., Feng, Y., 2021. Response of exoelectrogens centered consortium to nitrate on collaborative metabolism, microbial community, and spatial structure. Chemical Engineering Journal 426, 130975. https://doi.org/10.1016/j.cej.2021.130975

Logan, B.E., Rossi, R., Ragab, A., Saikaly, P.E., 2019. Electroactive microorganisms in bioelectrochemical systems. Nature Reviews Microbiology 17, 307–319. https://doi.org/10.1038/s41579-019-0173-x

Lu, S., Hu, H., Sun, Y., Yang, J., 2009. Effect of carbon source on the denitrification in constructed wetlands. Journal of Environmental Sciences 21, 1036–1043. https://doi.org/10.1016/S1001-0742(08)62379-7

Lust, R., Nerut, J., Kasak, K., Mander, Ü., 2020. Enhancing Nitrate Removal from Waters with Low Organic Carbon Concentration Using a Bioelectrochemical System—A Pilot-Scale Study. Water 12, 516. https://doi.org/10.3390/w12020516

Margat, J., Gun, J. van der, 2013. Groundwater around the World, 0 ed. CRC Press. https://doi.org/10.1201/b13977

Moissl-Eichinger, C., Pausan, M., Taffner, J., Berg, G., Bang, C., Schmitz, R.A., 2018. Archaea Are Interactive Components of Complex Microbiomes. Trends in Microbiology 26, 70–85. https://doi.org/10.1016/j.tim.2017.07.004

Molognoni, D., Devecseri, M., Cecconet, D., Capodaglio, A.G., 2017. Cathodic groundwater denitrification with a bioelectrochemical system. Journal of Water Process Engineering 19, 67–73. https://doi.org/10.1016/j.jwpe.2017.07.013

Nguyen, V.K., Hong, S., Park, Y., Jo, K., Lee, T., 2015. Autotrophic denitrification performance and bacterial community at biocathodes of bioelectrochemical systems with either abiotic or biotic anodes. Journal of Bioscience and Bioengineering 119, 180–187. https://doi.org/10.1016/j.jbiosc.2014.06.016

Park, H.I., Kim, D. kun, Choi, Y.-J., Pak, D., 2005. Nitrate reduction using an electrode as direct electron donor in a biofilm-electrode reactor. Process Biochemistry 40, 3383–3388. https://doi.org/10.1016/j.procbio.2005.03.017

Pous, N., Koch, C., Colprim, J., Puig, S., Harnisch, F., 2014. Extracellular electron transfer of biocathodes: Revealing the potentials for nitrate and nitrite reduction of denitrifying microbiomes dominated by Thiobacillus sp. Electrochemistry Communications 49, 93–97. https://doi.org/10.1016/j.elecom.2014.10.011

Pous, N., Puig, S., Dolors Balaguer, M., Colprim, J., 2015. Cathode potential and anode electron donor evaluation for a suitable treatment of nitrate-contaminated groundwater in bioelectrochemical systems. Chemical Engineering Journal 263, 151–159. https://doi.org/10.1016/j.cej.2014.11.002

Pous, N., Carmona-Martínez, A. A., Vilajeliu-Pons, A., Fiset, E., Bañeras, L., Trably, E., et al. 2016. Bidirectional microbial electron transfer: Switching an acetate oxidizing biofilm to nitrate reducing conditions. Biosensor Bioelectronics 75, 352–358. doi: 10.1016/j.bios.2015.08.035

Pous, N., Puig, S., Balaguer, M.D., Colprim, J., 2017. Effect of hydraulic retention time and substrate availability in denitrifying bioelectrochemical systems. Environmental Science: Water Research and Technology 3, 922–929. https://doi.org/10.1039/C7EW00145B

Qambrani, N.A., Oh, S.-E., 2013. Effect of Dissolved Oxygen Tension and Agitation Rates on Sulfur-Utilizing Autotrophic Denitrification: Batch Tests. Applied Biochemistry and Biotechnology 169, 181–191. https://doi.org/10.1007/s12010-012-9955-6

Rahimi, S., Modin, O., Roshanzamir, F., Neissi, A., Saheb Alam, S., Seelbinder, B., Pandit, S., Shi, L., Mijakovic, I., 2020. Co-culturing Bacillus subtilis and wastewater microbial community in a bio-electrochemical system enhances denitrification and butyrate formation. Chemical Engineering Journal 397, 125437. https://doi.org/10.1016/j.cej.2020.125437

Rockström, J., Steffen, W., Noone, K., Persson, Å., Chapin, F.S., Lambin, E.F., Lenton, T.M., Scheffer, M., Folke, C., Schellnhuber, H.J., Nykvist, B., de Wit, C.A., Hughes, T., van der Leeuw, S., Rodhe, H., Sörlin, S., Snyder, P.K., Costanza, R., Svedin, U., Falkenmark, M., Karlberg, L., Corell, R.W., Fabry, V.J., Hansen, J., Walker, B., Liverman, D., Richardson, K., Crutzen, P., Foley, J.A., 2009. A safe operating space for humanity. Nature 461, 472–475. https://doi.org/10.1038/461472a

Rousseau, R., Etcheverry, L., Roubaud, E., Basséguy, R., Délia, M.-L., Bergel, A., 2020. Microbial electrolysis cell (MEC): Strengths, weaknesses and research needs from electrochemical engineering standpoint. Applied Energy 257, 113938. https://doi.org/10.1016/j.apenergy.2019.113938

Schalk, J., de Vries, S., Kuenen, J.G., Jetten, M.S.M., 2000. Involvement of a Novel Hydroxylamine Oxidoreductase in Anaerobic Ammonium Oxidation. Biochemistry 39, 5405–5412. https://doi.org/10.1021/bi992721k

Song, B., Lisa, J.A., Tobias, C.R., 2014. Linking DNRA community structure and activity in a shallow lagoonal estuarine system. Frontiers in Microbiology 5.

Sparacino-Watkins, C., Stolz, J.F., Basu, P., 2013. Nitrate and periplasmic nitrate reductases. Chemistry Society Reviews 43, 676–706. https://doi.org/10.1039/C3CS60249D

Su, D., Chen, Y., 2022. Advanced bioelectrochemical system for nitrogen removal in wastewater. Chemosphere 292, 133206. https://doi.org/10.1016/j.chemosphere.2021.133206

Van Doan, T., Lee, T.K., Shukla, S.K., Tiedje, J.M., Park, J., 2013. Increased nitrous oxide accumulation by bioelectrochemical denitrification under autotrophic conditions: kinetics and expression of denitrification pathway genes. Water Research 47, 7087–7097. https://doi.org/10.1016/j.watres.2013.08.041

Virdis, B., Rabaey, K., Yuan, Z., Keller, J., 2008. Microbial fuel cells for simultaneous carbon and nitrogen removal. Water Research 42, 3013–3024. https://doi.org/10.1016/j.watres.2008.03.017

Virdis, B., Rabaey, K., Rozendal, R.A., Yuan, Z., Keller, J., 2010. Simultaneous nitrification, denitrification and carbon removal in microbial fuel cells. Water Research 44, 2970–2980. https://doi.org/10.1016/j.watres.2010.02.022

Wang, M., Huang, G., Zhao, Z., Dang, C., Liu, W., Zheng, M., 2018. Newly designed primer pair revealed dominant and diverse comammox amoA gene in full-scale wastewater treatment plants. Bioresource Technology 270, 580–587. https://doi.org/10.1016/j.biortech.2018.09.089

Wang, X., Prévoteau, A., Rabaey, K., 2021a. Impact of Periodic Polarization on Groundwater Denitrification in Bioelectrochemical Systems. Environmental Science and Technology 55, 15371–15379. https://doi.org/10.1021/acs.est.1c03586

Wang, H., Yang, Q., Yan, Q., Wen, Q., 2021b. Primary insight into the cathode strengthened electrons transport and nitrous oxide reduction during hydrogenotrophic denitrification in bioelectrochemical system (BES). Journal of Environmental Chemical Engineering 9, 104723. https://doi.org/10.1016/j.jece.2020.104723

Xu, Dan, Xiao, E., Xu, P., Zhou, Y., He, F., Zhou, Q., Xu, Dong, Wu, Z., 2017. Performance and microbial communities of completely autotrophic denitrification in a bioelectrochemically-assisted constructed wetland system for nitrate removal. Bioresource Technology 228, 39–46. https://doi.org/10.1016/j.biortech.2016.12.065

Xue, L., Chen, N., Tong, S., Yang, C., Feng, C., 2022. Bioelectrochemical reactor improved by assembling anode with rice husk for treating nitrate-contaminated groundwater. Journal of Water Process Engineering 47, 102778. https://doi.org/10.1016/j.jwpe.2022.102778

Yang, Q., Zhao, H., Liang, H., 2015. Denitrification of overlying water by microbial electrochemical snorkel. Bioresource Technology 197, 512–514. https://doi.org/10.1016/j.biortech.2015.08.127

Yang, X.-L., Zang, L., Chen, J.-J., Xu, H., Yang, Y.-J., Song, H.-L., 2023. Nitrogen removal enhanced by its migration and transformation in a three-chamber microbial electrolysis cell. Journal of Water Process Engineering 53, 103683. https://doi.org/10.1016/j.jwpe.2023.103683

Yu, L., Yuan, Y., Chen, S., Zhuang, L., Zhou, S., 2015. Direct uptake of electrode electrons for autotrophic denitrification by Thiobacillus denitrificans. Electrochemistry Communications 60, 126–130. https://doi.org/10.1016/j.elecom.2015.08.025

Zhang, L., Jiang, M., Zhou, S., 2022. Conversion of nitrogen and carbon in enriched paddy soil by denitrification coupled with anammox in a bioelectrochemical system. Journal of Environmental Sciences 111, 197–207. https://doi.org/10.1016/j.jes.2021.03.033

Zhao, T., Xie, B., Yi, Y., Zang, Y., Liu, H., 2023. Two polarity reversal modes lead to different nitrate reduction pathways in bioelectrochemical systems. Science of The Total Environment 856, 159185. https://doi.org/10.1016/j.scitotenv.2022.159185

Zhu, G., Onodera, T., Tandukar, M., Pavlostathis, S.G., 2013. Simultaneous carbon removal, denitrification and power generation in a membrane-less microbial fuel cell. Bioresource Technology 146, 1–6. https://doi.org/10.1016/j.biortech.2013.07.032

Zhu, C., Wang, H., Yan, Q., He, R., Zhang, G., 2017. Enhanced denitrification at biocathode facilitated with biohydrogen production in a three-chambered bioelectrochemical system (BES) reactor. Chemical Engineering Journal 312, 360–366. https://doi.org/10.1016/j.cej.2016.11.152

Zhou, S., Huang, S., He, J., Li, H., Zhang, Y., 2016. Electron transfer of Pseudomonas aeruginosa CP1 in electrochemical reduction of nitric oxide. Bioresource Technology 218, 1271–1274. https://doi.org/10.1016/j.biortech.2016.07.010

SUMMARY IN ESTONIAN

Mikrobioloogiliste ja keskkonnategurite mõju nitraadi eemaldamisele veest bioelektrokeemilistes süsteemides

Maapiirkondades on üheks peamiseks keskkonna saastumise probleemiks üleväetamisest ja lämmastiku kadudest tingitud kõrge nitraadisisaldus vees, mis paljudes kohtades ületab EL kehtestatud piirnorme, tehes selle vee tarbimise tervisele ohtlikuks. Seetõttu on oluline leida viise ülemääraselt saastunud vee puhastamiseks. Tänu keerulisele tsüklile ja erinõuetele on nitraadi (NO_3^-) eemaldamine veest kallis ning energiamahukas. Seetõttu pakuvad bioelektrokeemilised süsteemid (BES) erilist huvi, kuna varasematest uuringutest on selgunud nende kõrge potentsiaal NO_3^- edukaks töötlemiseks ja veest täielikuks eemaldamiseks. BES-i efektiivsus NO_3^- eemaldamisel sõltub suuresti mikroobide aktiivsusest ja ehkki BES-i disaini on suures osas uuritud, on teadmised mikrobioomi rolli kohta endiselt piiratud.

Käesolevas töös analüüsiti lämmastiku (N) aineringe kontrollgeenide arvukust, määramaks kindlaks levinud protsessid, mis vastutavad NO_3^- eemaldamise eest BES-is. Uuriti mikroobseid elektrokeemilisi snorkelsüsteeme (MES), et selgitada katoodi materjali ja selle pindala mõju NO_3^- transformatsiooni kiirusele. MESi efektiivsuse ja jätkusuutlikkuse iseloomustamiseks analüüsiti naerugaasi (N_2O) voogusid, N transformeerivate geenide arvukuse muutumist, vee ja sette füüsikalis-keemilisi parameetreid, samuti redokspotentsiaali tsüklilise voltammeetria abil. MES-i NO_3^- eemaldamise efektiivsus oli vahemikus 40% kuni 70%, nitritil (NO_2^-) ~98%. Katoodi ja anoodi ühendamine (snorkel-süsteemi tähenduses lühises) vähendas oluliselt geenide arvukust, muutes vastavalt ka mikroobide aktiivsust. Grafiitvildi kasutamine katoodimaterjalina toetas nitrifitseerivaid prokarüoote, kuid piiras *nirK* geeni omavate denitrifitseerijate arvukust. Anaeroobse ammooniumi oksüdatsiooni (ANAMMOX) aktiivsus näitas kontrollrühmaga võrreldes langust. Suuremad N_2O vood mõõdeti katood:anood töötlusega vahekorras 1:1, kasutades katoodimaterjalidena nii grafiitvilti, vaske, plasti kui ka roostevaba terast. *nirS* (N_2O tootja) ja *nosZI* (N_2O tarbija) geenide arvukus suurenes MES süsteemis oluliselt. Dissimileeriv redutseerimine ammooniumiks (DNRA) võib samuti olla N_2O emisiooni eest, sest *nrfA* geenide arvukus tõusis elektrokeemilise manipuleerimisega.

NO_3^- eemaldamine madala süsinikusisaldusega ühekambrilise mikroobse elektrosünteesi reaktoris (MESR) oli stabiilne, kuid suhteliselt madal. Suurem võrdluselektroodi (CE) potentsiaal võrreldes tööelektroodiga (WE) säilitas süsteemis pH-d (~7,3) ja hoidis madalamat hapniku (O_2) kontsentratsiooni. NO_3^- lähtekontsentratsiooni suurendamine ning CE potentsiaali tõstmine −756 mV-ni algatasid NO_3^- kiire vähenemise MESR-is. Maksimaalne NO_3^- — eemaldamise kiirus 3,8±1,2 mg NO_3^--N L^{-1} d^{-1} saavutati −656 mV ning 71% Faraday efektiivsuse juures. *nir* ja *nosZ* geenide arvukus oli WE-s suurem kui CE-s, mis näitab denitrifitseerijate olulisust süsteemis, mistõttu denitrifikatsiooniprotsess on tõenäoliselt vastutav NO_3^- eemaldamise eest süsteemis.

MESR-i madala süsinikusisalduse tõttu oli selles heterotroofsete mikroobide osakaal vaid ~5%, mis viitab protsessi juhtivale autotroofsele denitrifikatsioonile. MESR-is täheldati ka DNRA protsessi, mis tõenäoliselt põhjustas ~45% NO_3^- muutumisest NH_3^--ks. Seda näitab ka DNRA kontrollgeeni *nrfA* suhteliselt kõrge arvukus WE-s.

Kirjandusele baseeruvas ülevaateartiklis analüüsiti BES-i komponente ja tööparameetreid ning nende rolli NO_3^- eemaldamisel. Viimase hindamisel võeti arvesse erinevaid tegureid, sealhulgas elektroodide materjali, süsteemi töörežiimi, kambrite arvu, inokulaadi tüüpi, mahtu ja mikroobikoosluse struktuuri. Elektroodide materjal mõjutas NO_3^- eemaldamise kiirust kõige enam. Kasutades *random forest*'i klassifitseerimisalgoritmi leiti, et ka töörežiimi, kambrite arvu, inokulaadi tüübi ja süsteemi mahu mõju NO_3^- eemaldamise efektiivsusele on statistiliselt oluline. NO_3^--ga saastunud vee töötlemisel BES-is domineerisid prokarüootide hõimkonnad *Proteobacteria* ja *Firmicutes*. Ülevaateartiklis leiti, et lisaks denitrifikatsiooniprotsessile, mida iseloomustavad *narG*, *nirS*, *nirK*, no*sZI* ja *nosZII* geenide rohkus, oli tõendeid ANAMMOX protsessi kohta *hzsB* (ANAMMOX-spetsiifiliste 16S rRNA geeni) arvukuse kaudu. Ka varasemates töödes täheldati *nrfA* geeni alusel DNRA rolli olulisust NO_3^- eemaldamisel BES-is. Käesoleva töö analüüsi põhjal aitaks läbivooluline kahekambriline BES-süsteem, mille katoodi- ja anoodimaterjalina on granuleeritud süsinik ja süsinikpaber ning inokulaaditüübina denitrifitseerivad mikroobid, tagada optimaalse NO_3^- eemaldamise efektiivsuse.

Denitrifitseerijad osutusid elektrokeemilise manipuleerimise suhtes vastupidavamateks kui teised N aineringe kontrollgeenid. Tõenäoliselt on BES-is olulisim roll täielikul denitrifikatsioonil, mille käigus lendub atmosfääri molekulaarne lämmastik (N_2), mis on õhu peamine koostisosa. Tuleviku perspektiivina on mõeldav ka BES-i kasutamine täiustatud DNRA abil ammoniaaklämmastiku (NH_3-N) tootmiseks vähendades sünteetilise lämmastikväetiste tootmise vajadust.

Kokkuvõttes võib öelda, et BES saab kasutada edukaks NO_3^- eemaldamiseks süsinikuvaeses vees, näiteks põhjavees, aga ka kõrgema kontsentratsiooniga reovete järelpuhastamiseks.

ACKNOWLEDGEMENTS

I would like to thank my supervisors, Prof. Ülo Mander and Assoc. Prof. Mikk Espenberg, for all the guidance throughout my journey as a student. They aided my growth as a young researcher, and their directions have led me to achieve my academic goals. I still wonder how Ülo found my email and replied to me, now that I know the volume of mail he receives and how few of them capture his attention. Mikk has been the mentor who led the breadcrumbs for me, which I just had to follow to achieve my research goals. There have been waves of intimidation and excitement throughout this journey, and I am glad I was understood. I have eagerly awaited approval for all my work. I would like to thank all the people and staff of the Department of Geography who were warm and answered all my silly questions and helped me when I had doubts. To each one of them who aided my research and supported my studies, including all the technicians and researchers.

This time has been the most crucial and dynamic period in my life, and many drastic changes have occurred during this time, whether it was moving out of the country, committing to a PhD program abroad, acclimatizing to the quaintness and quietness, pandemic, and even the prominent appearance of a permanent wrinkle on my forehead.

I had to create chaos around me to thrive and eventually become comfortable with the silence.

My parents, a strong backbone I can rely on for the freedom of thought and utmost encouragement as my nurturers. My dad hasn't missed a day without wishing me "Good Morning" since I moved out of our home; he uses it as a way to check if I am alive! My Mummy, for the brave heart that she is, I have seen her learning new skills at all stages of her life. My sister, for the nuisance that she is, which makes me feel good about myself. My partner, Sharan, a fierce egalitarian, I am grateful for our close-to-perfect equal partnership and for being my biggest cheerleader. The extended family, who have taken care of me, and being around them influenced me to pursue science.

There have been moments of doubt, and I have contemplated learning to knit and sell hair bows. I'm glad everyone helped me swing through.

To my peers and friends, to Janaki and Sachin, distance wouldn't keep our friendship at bay. To the great friends I made in Tartu, Qurat, for being a big sister to me here and trying very hard to protect me.

To my mentor, Prof. Srikanth Mutnuri, who has guided me through my career and is responsible for helping me align my interests with applied environmental biotechnology and providing me with valuable experiences.

Lastly, to all the movies, books, and music that have been constant companions and nourishment for my soul.

I came in as a pompous, wish-to-know-it-all kind of young curious science enthusiast, and now I realize how much I did not know, and maybe would never know, and have to accept that because, as the famous Heraclitus said, feeling like an imposter is the only constant.

APPENDIX

Table. A. Parameters classified for analysis and removal of nitrate rate normalized to a common unit (mg liter^{-1} day^{-1}). The letters after the removal of nitrate rate are showing the differences between studies if other parameters were the same in the table (**a** – anode condition (abiotic, biotic), circuit connection; **b** – substrate (NO_3^- , NO_2^- +NO_3^-); **c** – proportion of cathodes embedded in simulated aquifier (0%, 100%); **d** – cathode potential (V); **e** – cathodic nitrate loading rate; **f** – hydraulic retention time (HRT), potential; **g** – carbon sources; **h** – chronoamperometry; **i** – circuit connection; **j** – C/N ratio; **k** – polarization (periodic, continuous); **l** – C/N ratio, HRT; **m** – inversion times (12, 24 and 48h)). *Capacity (<1L=I, 1–3L=II, >3L=III)

Study	Working mode	Type of inoculum	Cathode material	Anode material	Number of chambers	Capacity *	Volume (L)	Removal nitrate rate (mg L^{-1} day^{-1})
Chen et al., 2021	Continuous	Sediment	Combination	Combination	one	I	0.17	23.52
Nguyen et al., 2015	Batch	Activated sludge	Carbon felt	Carbon felt	two	I	0.7	0.63 **a**
Nguyen et al., 2015	Batch	Activated sludge	Carbon felt	Carbon felt	two	I	0.7	1.53 **a**
Nguyen et al., 2015	Batch	Activated sludge	Carbon felt	Carbon felt	two	I	0.7	1.56 **a**
Nguyen et al., 2015	Batch	Activated sludge	Carbon felt	Carbon felt	two	I	0.7	2.39 **a**
Nguyen et al., 2015	Batch	Activated sludge	Carbon felt	Carbon felt	two	I	0.7	1.7 **a**
Nguyen et al., 2015	Batch	Activated sludge	Carbon felt	Carbon felt	two	I	0.7	1.4 **a**
Nguyen et al., 2015	Batch	Activated sludge	Carbon felt	Carbon felt	two	I	0.7	1.51 **a**
Kondaveeti et al., 2014	Fed-Batch	Activated sludge	Carbon paper	Carbon paper	two	I	0.4	204 **b**
Kondaveeti et al., 2014	Fed-Batch	Activated sludge	Carbon paper	Carbon paper	two	I	0.4	188 **b**
Pous et al., 2016	Fed-Batch	Activated sludge	Carbon rod	Carbon rod	two	II	1	0.345
Nguyen et al., 2016	Batch	Activated sludge	Carbon felt	Carbon felt	two	I	0.7	0.831 **c**
Nguyen et al., 2016	Batch	Activated sludge	Carbon felt	Carbon felt	two	I	0.7	0.322 **c**
Pous et al., 2015	Fed-Batch	Uninoculated	Carbon granules	Carbon granules	one	II	1.05	65.279 **d**
Pous et al., 2015	Fed-Batch	Uninoculated	Carbon granules	Carbon granules	one	II	1.05	113.75 **d**
Al Mamun et al., 2017	Continuous	Activated sludge	Combination	Combination	three	II	1.8	24.59 **e**
Al Mamun et al., 2017	Continuous	Activated sludge	Combination	Combination	three	II	1.8	50.28 **e**
Al Mamun et al., 2017	Continuous	Activated sludge	Combination	Combination	three	II	1.8	76.8 **e**
Al Mamun et al., 2017	Continuous	Activated sludge	Combination	Combination	three	II	1.8	100.21 **e**
Al Mamun et al., 2017	Continuous	Activated sludge	Combination	Combination	three	II	1.8	117.32 **e**

Study	Working mode	Type of inoculum	Cathode material	Anode material	Number of chambers	Capacity *	Volume (L)	Removal nitrate rate (mg L^{-1} day^{-1})
Al Mamun et al., 2017	Continuous	Activated sludge	Combination	Combination	three	II	1.8	136.17 **e**
Al Mamun et al., 2017	Continuous	Activated sludge	Combination	Combination	three	II	1.8	150.1 **e**
Al Mamun et al., 2017	Continuous	Activated sludge	Combination	Combination	three	II	1.8	141.4 **e**
Al Mamun et al., 2017	Continuous	Activated sludge	Combination	Combination	three	II	1.8	122 **e**
Kondaveeti et al., 2019	Continuous	Activated sludge	Carbon fiber	Carbon fiber	two	I	0.5	26 **f**
Kondaveeti et al., 2019	Continuous	Activated sludge	Carbon fiber	Carbon fiber	two	I	0.5	50 **f**
Kondaveeti et al., 2019	Continuous	Activated sludge	Carbon fiber	Carbon fiber	two	I	0.5	64 **f**
Kondaveeti et al., 2019	Continuous	Activated sludge	Carbon fiber	Carbon fiber	two	I	0.5	96 **f**
Kondaveeti et al., 2019	Continuous	Activated sludge	Carbon fiber	Carbon fiber	two	I	0.5	56 **f**
Kondaveeti et al., 2019	Continuous	Activated sludge	Carbon fiber	Carbon fiber	two	I	0.5	78 **f**
Kondaveeti et al., 2019	Continuous	Activated sludge	Carbon fiber	Carbon fiber	two	I	0.5	114 **f**
Pous et al., 2017	Fed-Batch	Denitrifying microbes	Combination	Combination	two	II	2.5	849
Feng et al., 2013	Batch	Activated sludge	Carbon rod	Carbon rod	one	I	0.45	10.56 **g**
Feng et al., 2013	Batch	Activated sludge	Carbon rod	Carbon rod	one	I	0.45	22.8 **g**
Feng et al., 2013	Batch	Activated sludge	Carbon rod	Carbon rod	one	I	0.45	24 **g**
Feng et al., 2013	Batch	Activated sludge	Carbon rod	Carbon rod	one	I	0.45	26.16 **g**
Tong et al.,2013	Continuous	Activated sludge	Combination	Carbon fiber	two	I	0.25	208.2
Pous et al., 2014	Fed-Batch	Denitrifying microbes	Carbon rod	Carbon rod	one	I	0.018	2.64 **h**
Pous et al., 2014	Fed-Batch	Denitrifying microbes	Carbon rod	Carbon rod	one	I	0.018	1.62 **h**
Pous et al., 2014	Fed-Batch	Denitrifying microbes	Carbon rod	Carbon rod	one	I	0.018	2.78 **h**
Fang et al., 2022	Batch	CW Sediment	Stainless Steel	Stainless Steel	CW-BES	II	1.575	0.5 **i**
Fang et al., 2022	Batch	CW Sediment	Stainless Steel	Stainless Steel	CW-BES	II	1.575	2.97 **i**
Huang et al., 2013	Batch	Activated sludge	Carbon rod	Carbon rod	one	I	0.45	16.56 **j**
Huang et al., 2013	Batch	Activated sludge	Carbon rod	Carbon rod	one	I	0.45	26.16 **j**
Lust et al., 2020	Batch	Activated sludge	Carbon cloth	Stainless Steel	two	III	5.86	1.4
Lust et al., 2022	Batch	Denitrifying microbes	Carbon cloth	Carbon felt	one	III	5.8	3.81
Cecconet et al., 2018	Continuous	Activated sludge	Combination	Stainless Steel	two	II	1.37	62.15
Clauwaert et al., 2007	Continuous	Activated sludge	Combination	Carbon rod	two	I	0.716	146

Study	Working mode	Type of inoculum	Cathode material	Anode material	Number of chambers	Capacity *	Volume (L)	Removal nitrate rate (mg L^{-1} day^{-1})
Virdis et al., 2008	Batch	Activated sludge	Carbon granules	Carbon rod	two	I	0.364	345
Virdis et al., 2010	Batch	Activated sludge	Carbon granules	Carbon rod	two	I	0.672	175
Zhu et al., 2013	Batch	Denitrifying microbes	Carbon cloth	Carbon cloth	one	II	2.43	186
Kondaveeti et al., 2013	Batch	Activated sludge	Carbon paper	Carbon paper	two	I	0.4	204
Wang et al., 2021a	Continuous	Denitrifying microbes	Carbon granules	Combination	two	I	0.35	233 **k**
Wang et al., 2021a	Continuous	Denitrifying microbes	Carbon granules	Combination	two	I	0.35	205 **k**
Van Doan et al., 2013	Continuous	Activated sludge	Carbon felt	Carbon rod	one	I	0.45	39.6
Gregory et al., 2004	Batch	Sediment	Carbon rod	Carbon rod	two	I	0.5	19.92
Park et al.,2005	Batch	Activated sludge	Carbon felt	Carbon mesh	two	II	1	170
Chen et al., 2016	Batch	Activated sludge	Carbon fiber	Combination	3D BES	II	3	0.85 **l**
Chen et al., 2016	Batch	Activated sludge	Carbon fiber	Combination	3D BES	II	3	1.08 **l**
Chen et al., 2016	Batch	Activated sludge	Carbon fiber	Combination	3D BES	II	3	1.07 **l**
Chen et al., 2016	Batch	Activated sludge	Carbon fiber	Combination	3D BES	II	3	0.98 **l**
Amanze et al., 2023	Fed-Batch	Denitrifying microbes	Carbon cloth	Carbon fiber	one	I	0.028	50 **e**
Amanze et al., 2023	Fed-Batch	Denitrifying microbes	Carbon cloth	Carbon fiber	one	I	0.028	100 **e**
Amanze et al., 2023	Fed-Batch	Denitrifying microbes	Carbon cloth	Carbon fiber	one	I	0.028	75 **e**
Guo et al., 2023	Batch	Activated sludge	Carbon paper	Stainless Steel	two	I	0.1	1.5 **m**
Guo et al., 2023	Batch	Activated sludge	Carbon paper	Stainless Steel	two	I	0.1	1.1 **m**
Guo et al., 2023	Batch	Activated sludge	Carbon paper	Stainless Steel	two	I	0.1	0.44 **m**
Kong et al., 2023	Batch	Activated sludge	Carbon fiber	Carbon fiber	two	I	0.43	48
Rahimi et al., 2020	Fed-Batch	Denitrifying microbes	Carbon rod	Carbon felt	two	I	0.1	48.4
Xu et al., 2017	Continuous	Activated sludge	Carbon felt	Carbon granules	CW-BES	III	25	3.53 **j**
Xu et al., 2017	Continuous	Activated sludge	Carbon felt	Carbon granules	CW-BES	III	25	5.47 **j**
Xue et al., 2022	Batch	Activated sludge	Stainless Steel	Stainless Steel	one	III	3.57	0.27
Yang et al., 2023	Continuous	Activated sludge	Carbon fiber	Combination	three	II	1.07	2.83

Table. B. Parameters classified for analysis with NO_3^- removal percentage (%). The letters after the removal of nitrate rate are showing the differences between studies if other parameters were the same in the table (**a** – pH; **b** – anode condition (abiotic, biotic), circuit connection; **c** – substrate (NO_3^- , NO_2^- +NO_3^-); **d** – facilitated cathode; **e** – HRT, cathode potential (V); **f** – substrate concentration; **g** – HRT, C/N ratio; **h** – HRT; **i** – facilitated cathode; **j** – size of cathode; **k** – pH; **l** – nitrate loading; **m** – inversion times (12, 24 and 48h)). *Capacity (<L=I, 1–3L=II, >3L=III)

Study	Working mode	Type of inoculum	Cathode material	Anode material	Number of chambers	Capa-city *	Volume (L)	Removal of nitrate (%)
Wang et al., 2018	Continuous	Activated sludge	Carbon fiber	Carbon rod	one	II	2.5	83.71 **a**
Wang et al., 2018	Continuous	Activated sludge	Carbon fiber	Carbon rod	one	II	2.5	97.21 **a**
Wang et al., 2018	Continuous	Activated sludge	Carbon fiber	Carbon rod	one	II	2.5	93 **a**
Chen et al., 2021	Continuous	Sediment	Combination	Carbon rod	one	I	0.17	51.5
Nguyen et al., 2015	Batch	Activated sludge	Carbon felt	Carbon felt	two	I	0.7	50 **b**
Nguyen et al., 2015	Batch	Activated sludge	Carbon felt	Carbon felt	two	I	0.7	43 **b**
Nguyen et al., 2015	Batch	Activated sludge	Carbon felt	Carbon felt	two	I	0.7	43 **b**
Nguyen et al., 2015	Batch	Activated sludge	Carbon felt	Carbon felt	two	I	0.7	28 **b**
Kondaveeti et al., 2014	Fed-Batch	Activated sludge	Carbon paper	Carbon paper	two	I	0.4	87.9 **c**
Kondaveeti et al., 2014	Fed-Batch	Activated sludge	Carbon paper	Carbon paper	two	I	0.4	85.4 **c**
Kondaveeti et al., 2014	Fed-Batch	Activated sludge	Carbon paper	Carbon paper	two	I	0.4	84.7 **c**
Liu et al., 2014	Batch	Denitrifying microbes	Carbon fiber	Carbon fiber	two	II	1.1	59 **d**
Liu et al., 2014	Batch	Denitrifying microbes	Carbon fiber	Carbon fiber	two	II	1.1	95 **d**
Molognoni et al., 2017	Continuous	Activated sludge	Carbon rod	Stainless Steel	two	II	1.43	90
Kondaveeti et al., 2019	Continuous	Activated sludge	Carbon fiber	Carbon fiber	two	I	0.5	94 **e**
Kondaveeti et al., 2019	Continuous	Activated sludge	Carbon fiber	Carbon fiber	two	I	0.5	85 **e**
Kondaveeti et al., 2019	Continuous	Activated sludge	Carbon fiber	Carbon fiber	two	I	0.5	74 **e**
Kondaveeti et al., 2019	Continuous	Activated sludge	Carbon fiber	Carbon fiber	two	I	0.5	65 **e**
Kondaveeti et al., 2019	Continuous	Activated sludge	Carbon fiber	Carbon fiber	two	I	0.5	96 **e**
Kondaveeti et al., 2019	Continuous	Activated sludge	Carbon fiber	Carbon fiber	two	I	0.5	91 **e**

Study	Working mode	Type of inoculum	Cathode material	Anode material	Number of chambers	Capa-city *	Volume (L)	Removal of nitrate (%)
Kondaveeti et al., 2019	Continuous	Activated sludge	Carbon fiber	Carbon fiber	two	I	0.5	81 **e**
Zhang et al., 2022	Batch	Sediment	Carbon rod	Carbon rod	two	I	0.06	64 **f**
Zhang et al., 2022	Batch	Sediment	Carbon rod	Carbon rod	two	I	0.06	84 **f**
Zhang et al., 2022	Batch	Sediment	Carbon rod	Carbon rod	two	I	0.06	84 **f**
Yang et al., 2015	Batch	Sediment	Iron rod	Carbon felt	one	II	2	98
Hao et al., 2013	Continuous	Activated sludge	Carbon rod	Carbon rod	one	III	3.4	98.3 **g**
Hao et al., 2013	Continuous	Activated sludge	Carbon rod	Carbon rod	one	III	3.4	88.4 **g**
Pous et al., 2017	Fed-Batch	Denitrifying microbes	Combination	Combination	two	II	2.5	100 **h**
Pous et al., 2017	Fed-Batch	Denitrifying microbes	Combination	Combination	two	II	2.5	55 **h**
Pous et al., 2017	Fed-Batch	Denitrifying microbes	Combination	Combination	two	II	2.5	94 **h**
Pous et al., 2017	Fed-Batch	Denitrifying microbes	Combination	Combination	two	II	2.5	50 **h**
Zhu et al., 2017	Batch	Activated sludge	Carbon fiber	Carbon fiber	two	II	2.24	95 **i**
Zhu et al., 2017	Batch	Activated sludge	Carbon fiber	Carbon fiber	two	II	2.24	95 **i**
Zhu et al., 2017	Batch	Activated sludge	Carbon fiber	Carbon fiber	three	II	2.24	95 **i**
Gadegaonkar et al., 2020	Batch	CW Sediment	None	Carbon felt	one	II	2	53.88 **j**
Gadegaonkar et al., 2020	Batch	CW Sediment	Carbon felt	Carbon felt	one	II	2	48.39 **j**
Gadegaonkar et al., 2020	Batch	CW Sediment	Carbon felt	Carbon felt	one	II	2	41.35 **j**
Gadegaonkar et al., 2020	Batch	CW Sediment	Carbon felt	Carbon felt	one	II	2	41.52 **j**
Gadegaonkar et al., 2020	Batch	CW Sediment	Carbon felt	Carbon felt	one	II	2	41.18 **j**
Gadegaonkar et al., 2020	Batch	CW Sediment	Stainless Steel	Carbon felt	one	II	2	40.34 **j**
Gadegaonkar et al., 2020	Batch	CW Sediment	Copper	Carbon felt	one	II	2	40.55 **j**
Gadegaonkar et al., 2020	Batch	CW Sediment	Plastic	Carbon felt	one	II	2	74.61 **j**
Chen et al., 2016	Batch	Activated sludge	Carbon fiber	Combination	3D-BES	II	3	77.12 **k**
Chen et al., 2016	Batch	Activated sludge	Carbon fiber	Combination	3D-BES	II	3	97.58 **k**
Chen et al., 2016	Batch	Activated sludge	Carbon fiber	Combination	3D-BES	II	3	96.36 **k**
Chen et al., 2016	Batch	Activated sludge	Carbon fiber	Combination	3D-BES	II	3	88.48 **k**

Study	Working mode	Type of inoculum	Cathode material	Anode material	Number of chambers	Capa-city *	Volume (L)	Removal of nitrate (%)
Chen et al., 2018	Batch	Activated sludge	Combination	Carbon rod	one	II	2.35	96.55
Amanze et al., 2023	Fed-Batch	Denitrifying microbes	Carbon cloth	Carbon fiber	one	I	0.028	98.92 **l**
Amanze et al., 2023	Fed-Batch	Denitrifying microbes	Carbon cloth	Carbon fiber	one	I	0.028	97 **l**
Amanze et al., 2023	Fed-Batch	Denitrifying microbes	Carbon cloth	Carbon fiber	one	I	0.028	48.98 **l**
Guo et al., 2023	Batch	Activated sludge	Carbon paper	Stainless Steel	two	I	0.1	54 **m**
Guo et al., 2023	Batch	Activated sludge	Carbon paper	Stainless Steel	two	I	0.1	40 **m**
Guo et al., 2023	Batch	Activated sludge	Carbon paper	Stainless Steel	two	I	0.1	16 **m**
Kong et al., 2023	Batch	Activated sludge	Carbon fiber	Carbon fiber	two	I	0.43	96
Rahimi et al., 2020	Fed-Batch	Denitrifying microbes	Carbon rod	Carbon felt	two	I	0.1	96.8
Xu et al., 2017	Continuous	Activated sludge	Carbon felt	Carbon granules	CW-BES	III	25	58.9 **g**
Xu et al., 2017	Continuous	Activated sludge	Carbon felt	Carbon granules	CW-BES	III	25	91.26 **g**
Xue et al., 2022	Batch	Activated sludge	Stainless Steel	Stainless Steel	one	III	3.57	99
Yang et al., 2023	Continuous	Activated sludge	Carbon fiber	Combination	three	II	1.07	72.9

Table. C. The table displays predominant Phylum, Class and Species observed in BES utilized for NO_3^- removal. (ND – no data).

Citation	Predominant phylum	Class	Species	Rate of nitrate removal (mg liter^{-1} day^{-1}) or % nitrate removal
Kondaveeti et al., 2014	*Proteobacteria, Bacteroidetes, Actinobacteria, Firmicutes*	*Gammaproteobacteria*	*Proteiniphilum acetatigenes, Weeksella virosa, Pseudomonas stutzeri, Thauera aromatica, Bacillus novalis*	196 mg liter^{-1} day^{-1}
Hao et al., 2013	*Proteobacteria, Firmicutes, Actinobacteria*	*Alphaproteobacteria, Betaproteobacteria, Gammaproteobacteria, Epislonproteobacteria, Clostridia, Bacilli*	ND	93.35%
Liu et al., 2014	*Bacterioidetes, Proteobacteria. Firmicutes, Actinobacteria*	*Alphaproteobacteria, Betaproteobacteria, Gammaproteobacteria, Epislonproteobacteria, Clostridia, Bacilli*	*Thauera terpenica*	77%
Nguyen et al., 2015	ND	ND	*Pseudomonas oleovorans, Aeromonas, Curtobacterium*	1.53 mg liter^{-1} day^{-1}
Pous et al., 2014	ND	*Betaproteobacteria*	*Thiobacillus thiophilus*	2.34 mg liter^{-1} day^{-1}
Pous et al., 2015	ND	ND	*Geobacter*	89.51 mg liter^{-1} day^{-1}
Yang et al., 2015	ND	ND	*Lysinibacillus, Ochrobactrum, Pseudomonas, Aeromonas*	98%
Zhu et al., 2017	*Proteobacteria, Chloroflexi, Bacteroidetes, Firmicutes*	ND	ND	95%

Citation	Predominant phylum	Class	Species	Rate of nitrate removal (mg liter^{-1} day^{-1}) or % nitrate removal
Wang et al., 2018[a]	*Proteobacteria, Firmicutes, Actinobacteria, Bacteroidetes, Tenericutes, Chloroflexi, Acidobacteria, Fibrobacteres, Saccharibacteria*	*Gammaproteobacteria, Betaproteobacteria, Alphaproteobacteria, Bacilli, Clostridia, Erysipelotrichia, OPB54, Actinobacteria, Flavobacteriia, Spingobacteriia, Mollicutes, Anaerolineae, Acidobacteria, Fibrobacteria, Saccharibacteria_norank*	*Pseudomonas, Halomonas, Thauera*	87.71%
Wang et al., 2018[a]	*Proteobacteria, Firmicutes, Actinobacteria, Bacteroidetes, Tenericutes, Chloroflexi, Chrysiogenetes, SHA-109*	*Gammaproteobacteria, Betaproteobacteria, Alphaproteobacteria, Bacilli, Clostridia, Erysipelotrichia, OPB54, Flavobacteriia, Mollicutes, Anaerolineae, TK10, KD4-96, Chloroflexi_uncultured*	*Pseudomonas, Halomonas, Thauera*	97.21%
Wang et al., 2018[a]	*Proteobacteria, Firmicutes, Actinobacteria, Bacteroidetes, Tenericutes, Fibrobacteres, Verrucomicrobia, Chrysiogenetes*	*Gammaproteobacteria, Betaproteobacteria, Alphaproteobacteria, Proteobacteria_unclassified, Bacilli, Clostridia, Erysipelotrichia, OPB54, Flavobacteriia, Sphingobacteriia, Cytophagia, Mollicutes, Thermomicrobia, Chloroflexi_uncultured, Opitutae*	*Pseudomonas, Halomonas, Thauera*	93%

Citation	Predominant phylum	Class	Species	Rate of nitrate removal (mg liter^{-1} day^{-1}) or % nitrate removal
Yang et al., 2023	*Firmicutes, Actinobacteria, Armatimonadetes, Chloroflexi, Planetomycetes, Acidobacteria, Nitrospirae, Patescibacteria, Proteobacteria, Bacteroidetes, Epsilonbacteraeota*	*ND*	*ND*	2.83 mg liter^{-1} day^{-1}
Xu et al., 2017	*Proteobacteria, Euryarchaeota, Firmicutes, Elusimicrobia, Actinobacteria, Latescibacteria, Bacteroidetes, Ignavibacteriae, Planctomycetes, Candidatus Saccharibacteria, Chloroflexi, Gemmatimonadetes, Armatimonadetes, Fibrobacteres, Acidobacteria, Chlamydiae, Verrucomicrobia, Parcubacteria, Nitrospirae, Pacearchaeota, Spirochaetes, Candidatus Saccharibacteria, Verrucomicrobia*	*Gammaproteobacteria, Phycisphaerae, Betaproteobacteria, Acidobacteria_Gp4, Alphaproteobacteria, Acidobacteria_Gp16, Bacilli, Cytophagia, Epsilonproteobacteria, Opitutae, Actinobacteria, Nitrospira, Clostridia, Anaerolineae, Spingobacteriia, Erysipelotrichia, Deltaproteobacteria, Planctomycetia, Flavobacteriia, Chlamydiia, Bacteroidia*	*ND*	4.5 mg liter^{-1} day^{-1}
Xue et al., 2022	*Proteobacteria, Bacteroidetes, Firmicutes*	*ND*	*ND*	0.27 mg liter^{-1} day^{-1}

[a] Difference in pH

PUBLICATIONS

CURRICULUM VITAE

Name	Sharvari Sunil Gadegaonkar
Date of birth	23.12.1995
Citizenship	Indian
Email	sharvari@ut.ee

Education

2019–2023	University of Tartu, Faculty of Science and Technology, PhD studies in Environmental Technology
2017–2019	Birla Institute of Technology and Science, Pilani (BITS, Pilani), ME Biotechnology (Masters Engineering)
2013–2017	D.Y. Patil school of Biotechnology and Bioinformatics, BTech Biotechnology (Bachelors Technology)
2001–2013	Swami Vivekanand High school and Junior college

Scholarships

18.08–17.12.2021	Dora Plus short study visits support for mobility to University of Helsinki, Environmental soil science lab.

Teaching

2021–2023	Biotechnology in Environmental Management (LOOM. 02.293) Practical Course in Environmental Biotechnology and Ecotechnology (LOOM.02.294)

Leadership journey

03.05–07.05.2021	IETN PhDs' Course in Authentic Leadership, LUT University
01.04–23.12.2023	EIT Climate-KIC Leadership Journey, Summer School, Trinity College Dublin, Ireland.

Conference presentations

10.09–14.09.2021	10th International Symposium on Wetlands Pollutant Dynamics and Control, WETPOL 2021. "Denitrification, ANAMMOX and to lesser extend nitrification are the main processes for nitrogen removal in constructed wetland microbial electrochemical systems" (Online-Oral presentation)
26.06–30.06.2022	10th International Symposium on Ecosystem Behavoir, BIOGEOMON 2022, Tartu, Estonia. (Poster presentation)
06.11–10.11.2022	17th International Conference of the IWA Specialist Group on Wetland Systems for Water Pollution Control. Lyon, France. "Parameters affecting enhanced denitrification in Bio-electrochemical systems" (Poster presentation)

23.04.–28.04.2013 General Assembly of the European Geosciences Union, EGU 2023, Vienna, Austria. “Microbial and environmental factors influencing NO_3^- removal in Bio-electrochemical systems” (Poster presentation)

Publications

Gadegaonkar, S.S., Philippon, T., Rogińska, J., Mander, Ü., Maddison, M., Etienne, M., Barrière, F., Kasak, K., Lust, R., Espenberg, M. 2020. Effect of cathode material and its size on the abundance of nitrogen removal functional genes in microcosms of integrated bioelectrochemical-wetland systems. Soil Systems 4(3), 47; https://doi.org/10.3390/soilsystems4030047

Lust, R., Nerut, J., **Gadegaonkar, S.S.,** Kasak, K., Espenberg, M., Visnapuu, T., Mander, Ü. 2022. Single-chamber microbial electrosynthesis reactor for nitrate reduction from waters with a low electron donors’ concentration: from design and set-up to the optimal operating potential. Frontiers in Environmental Sciences 10, 938631. https://doi.org/10.3389/fenvs.2022.938631

Gadegaonkar, S.S., Mander, Ü., Espenberg, M. 2023. A state-of-the-art review and guidelines for enhancing nitrate removal in bio-electrochemical systems (BES). Journal of Water Process Engineering. https://doi.org/10.1016/j. jwpe. 2023.103788

Masta, M., Espenberg, M., **Gadegaonkar, S.S.,** Pärn, J., Sepp, H., Kirsimäe, K., Sgouridis, F., Müller, C., Mander, Ü. 2022. Integrated isotope and microbiome analysis indicate dominance of denitrification in N2O production after rewetting of drained fen peat Biogeochemistry. https://doi.org/10.1007/ s10533-022-00971-3

ELULOOKIRJELDUS

Nimi	Sharvari Sunil Gadegaonkar
Sünniaeg	23.12.1995
Kodakondsus	India
E-post	sharvari@ut.ee

Haridus

2019–2023	Tartu Ülikool, loodus- ja tehnoloogiateaduskond, Keskkonnatehnoloogia doktoriõpe
2017–2019	Birla Tehnoloogia- ja Teadusinstituut, Pilani (BITS, Pilani) ME biotehnoloogia (magistriõpe)
2013–2017	D.Y. Patili biotehnoloogia ja bioinformaatika kool, BTech biotehnoloogia (bakalaureuse tehnoloogia)
2001–2013	Swami Vivekanandi keskkool ja kolledž

Stipendiumid

18.08–17.12.2021	Dora Plusi lühiõppevisiitide mobiilsustoetus Helsingi Ülikool, Soome, Keskkonna mullateaduse labor.

Õpetamine

2021–2023	Biotehnoloogia keskkonnajuhtimises (LOOM.02.293) Keskkonnabiotehnoloogia ja ökotehnoloogia praktiline kursus (LOOM.02.294)

Täiendõpe

03.05–07.05.2021	IETN PhDs' Course in Authentic Leadership, LUT Ülikool
01.04–23.12.2023	EIT Climate-KIC Leadership Journey, suvekool, Trinity kolledž, Dublin, Iirimaa.

Konverentsi ettekanded

10.09–14.09.2021	10th International Symposium on Wetlands Pollutant Dynamics and Control, WETPOL 2021. "Denitrification, ANAMMOX and to lesser extend nitrification are the main processes for nitrogen removal in constructed wetland microbial electrochemical systems" (suuline (*online*) ettekanne)
26.06–30.06.2022	10th International Symposium on Ecosystem Behavior, BIOGEOMON 2022, Tartu, Estonia (stendiettekanne)
06.11–10.11.2022	17th International Conference of the IWA Specialist Group on Wetland Systems for Water Pollution Control. Lyon, France. "Parameters affecting enhanced denitrification in Bio-electrochemical systems" (stendiettekanne)

23.04.–28.04.2013 General Assembly of the European Geosciences Union, EGU 2023, Vienna, Austria. “Microbial and environmental factors influencing NO_3^- removal in Bio-electrochemical systems” (stendiettekanne)

Publikatsioonid

Gadegaonkar, S.S., Philippon, T., Rogińska, J., Mander, Ü., Maddison, M., Etienne, M., Barrière, F., Kasak, K., Lust, R., Espenberg, M. 2020. Effect of cathode material and its size on the abundance of nitrogen removal functional genes in microcosms of integrated bioelectrochemical-wetland systems. Soil Systems 4(3), 47; https://doi.org/10.3390/soilsystems4030047

Lust, R., Nerut, J., **Gadegaonkar, S.S.,** Kasak, K., Espenberg, M., Visnapuu, T., Mander, Ü. 2022. Single-chamber microbial electrosynthesis reactor for nitrate reduction from waters with a low electron donors’ concentration: from design and set-up to the optimal operating potential. Frontiers in Environmental Sciences 10, 938631. https://doi.org/10.3389/fenvs.2022.938631

Gadegaonkar, S.S., Mander, Ü., Espenberg, M. 2023 A state-of-the-art review and guidelines for enhancing nitrate removal in bio-electrochemical systems (BES). Journal of Water Process Engineering. https://doi.org/10.1016/j.jwpe.2023.103788

Masta, M., Espenberg, M., **Gadegaonkar, S.S.,** Pärn, J., Sepp, H., Kirsimäe, K., Sgouridis, F., Müller, C., Mander, Ü. 2022. Integrated isotope and microbiome analysis indicate dominance of denitrification in N_2O production after rewetting of drained fen peat Biogeochemistry. https://doi.org/10.1007/s10533-022-00971-3

DISSERTATIONES TECHNOLOGIAE CIRCUMIECTORUM UNIVERSITATIS TARTUENSIS

1. **Sille Teiter**. Emission rates of N_2O, N_2, CH_4 and CO_2 in riparian grey alder forests and subsurface flow constructed wetlands. Tartu, 2005, 134 p.
2. **Kaspar Nurk**. Relationships between microbial characteristics and environmental conditions in a horizontal subsurface flow constructed wetland for wastewater treatment. Tartu, 2005, 123 p.
3. **Märt Öövel**. Performance of wastewater treatment wetlands in Estonia. Tartu, 2006, 148 p.
   Sergei Yurchenko. Determination of some carcinogenic contaminants in food. Tartu, 2006, 143 p. Published in *Dissertation Chimicae Universitatis Tartuensis,* 51.
4. **Alar Noorvee**. The applicability of hybrid subsurface flow constructed wetland systems with re-circulation for wastewater treatment in cold climates. Tartu, 2007, 117 p.
   Ülle Jõgar. Conservation and restoration of semi-natural floodplain meadows and their rare plant species. Tartu, 2008, 99 p. Published in *Dissertation Biologicae Universitatis Tartuensis*, 139.
5. **Christina Vohla**. Phosphorus removal by various filter materials in subsurface flow constructed wetlands. Tartu, 2008, 103 p.
6. **Martin Maddison**. Dynamics of phytomass production and nutrient standing stock of cattail and its use for environment-friendly construction. Tartu, 2008, 87 p.
7. **Marika Truu**. Impact of land use on microbial communities in Estonian soils. Tartu, 2008, 126 p.
8. **Elar Põldvere**. Removal of organic material, nitrogen and phosphorus from wastewater in hybrid subsurface flow constructed wetlands. Tartu, 2009, 107 p.
9. **Margit Kõiv**. Treatment of landfill leachate and municipal wastewater in subsurface flow filters using mineralized peat and hydrated oil shale ash. Tartu, 2010, 147 p.
10. **Jaanis Juhanson**. Impact of phytoremediation and bioaugmentation on the microbial community in oil shale chemical industry solid waste. Tartu, 2010, 95 p.
    Aare Selberg. Evaluation of environmental quality in Northern Estonia by the analysis of leachate. Tartu, 2010, 117 p. Published in *Dissertation Chimicae Universitatis Tartuensis,* 99.
11. **Riho Mõtlep**. Composition and diagenesis of oil shale industrial solid wastes. Tartu, 2010, 127 p.
12. **Igor Zaytsev**. Bioaugmentation in LWA-filled horizontal subsurface flow filters for wastewater treatment: Impact of flow regime, temperature and donor system Tartu, 2010, 97 p.

13. **Siiri Velling**. Microbial BOD biosensor for wastewater analysis. Tartu, 2011, 79 p.
14. **Riina Lepik**. Biodegradability of phenolic compoundsas single and mixed substrates by activated sludge. Tartu, 2011, 153 p.
15. **Liis Marmor**. Ecology and bioindicative value of epiphytic lichens in relation to air pollution and forest continuity. Tartu, 2011, 98 p.
16. **Martin Liira**. Active filtration of phosphorus in Ca-rich hydrated oil shale ash: precipitation mechanisms and recovery. Tartu, 2012, 84 p.
17. **Kristjan Karabelnik**. Advanced design and management of hybrid constructed wetlands: environmental and water purification effects. Tartu, 2012, 128 p.
18. **Hiie Nõlvak**. Influence of qPCR workflow on target gene enumeration from environmental samples in the case of bioremediation potential estimation. Tartu, 2012, 136 p.
19. **Merlin Raud**. Study of semi-specific BOD biosensors for biosensor-array. Tartu, 2013, 103 p.
20. **Ivar Zekker**. Enrichment of anaerobic ammonium oxidizing bacteria for nitrogen removal from digester effluent and anammox process acceleration by intermediate compounds. Tartu, 2013, 142 p.
21. **Annika Uibopuu**. Communities of arbuscular mycorrhizal fungi in spruce forest ecosystem and their effect on performance of forest understorey plant species. Tartu, 2013, 104 p.
22. **Jekaterina Jefimova**. Leaching of polycyclic aromatic hydrocarbons (PAHs) and heavy metals from the oil shale processing wastes and from waste-based products. Tartu, 2015, 184 p.
23. **Teele Ligi**. Bacterial community structure and its genetic potential for nitrogen removal in the soils and sediments of a created riverine wetland complex. Tartu, 2015, 127 p.
24. **Kuno Kasak**. Greenhouse gas emissions and water treatment efficiency in subsurface flow filters using various substrates. Tartu, 2016, 128 p.
25. **Martin Ligi**. Application of close range remote sensing for monitoring aquatic environment. Tartu, 2017, 146 p.
26. **Mikk Espenberg**. Impact of management on peatland microbiome and greenhouse gas emissions. Tartu, 2017, 152 p.
27. **Jens-Konrad Preem**. Forest soil bacterial community analysis using high-throughput amplicon sequencing. Tartu, 2017, 108 p.
28. **Taavi Vaasma**. Enrichment, atmospheric dispersion and deposition of naturally occurring radionuclides from oil shale-fired power plants. Tartu, 2017, 175 p.
29. **Kristjan Oopkaup**. Microbial community and its relationship with pollutant removal in treatment wetlands. Tartu, 2018, 154 p.
30. **Ergo Rikmann**. Autotrophic nitrogen removal and relevant equilibrial processes. Tartu, 2019, 179 p.
31. **Kati Klein**. Studies and treatment of inhibitory and recalcitrant wastewater. Tartu, 2021, 168 p.

32. **Thomas Schindler**. Tree stem CH_4 and N_2O fluxes in various forest ecosystems. Tartu, 2021, 182 p.
33. **Peeter Paaver**. Development of alternative binders based on oil shale fly ash. Tartu, 2021, 130 p.
34. **Kertu Tiirik**. Antibiotic resistance in connected engineered and natural aquatic environments. Tartu, 2021, 124 p.
35. **Keit Kill**. Nutrient fluxes regulation in an in-stream constructed wetland treating polluted agricultural runoff. Tartu, 2022, 144 p.
36. **Rauno Lust**. Bioelectrochemical systems for enhanced removal of nitrate from water with a low electron donor concentration. Tartu, 2022, 145 p.
37. **Mihhail Fetissov**. Spatial decision support systems for ecosystem-based marine management. Tartu, 2022, 172 p.
38. **Mohit Masta**. Isotopologue and microbiome studies for N_2O source attribution in peat soils. Tartu, 2022, 113 p.
39. **Mirjam Uusõue**. Suspended particles dynamics and characteristics in optically complex waterbodies. Tartu, 2023, 144 p.